Pure Appl. Geophys. 173 (2016), 3795–3822

DOI 10.1007/s00024-016-1261-8

Pure and Applied Geophysics

Application and Comparison of Tsunami Vulnerability and Damage Models for the Town of Siracusa, Sicily, Italy

Gianluca Pagnoni[1] and Stefano Tinti[1]

Abstract—Siracusa is one of the most important cities of the eastern coast of Sicily, which according to historical records and to the present knowledge of the tectonic setting, is exposed to tsunamis generated by landslides on the Malta escarpment and by local and remote (e.g., Eastern Hellenic Arc) earthquakes. For this reason, the area of Siracusa has been selected as one of the test sites to conduct specific studies within the European FP7 project ASTARTE. In this frame, this work focuses on the assessment of tsunami vulnerability of (and damage to) the building stock of the town. The analysis is carried out following two different models, namely the SCHEMA and the Papathoma Tsunami Vulnerability Assessment (PTVA-3) methods. Topographic and building stock data in the potentially flooded areas are taken from detailed digital databases produced by the region of Sicily, integrated with satellite and photographic imagery from Google Earth and further validated by field surveys. We have explored three inundation scenarios corresponding to a constant-level tsunami flooding with assumed sea level rise of 1, 3 and 5 m, and evaluated the damage to the town buildings using both methods that make use of a 5-degree scale. The main result is that the level of damage of both models is not consistent, and that consistency may be improved if one changes from a 5- to a 3-degree damage scale.

Key words: Tsunami vulnerability assessment, tsunami damage assessment, buildings vulnerability, PTVA-3, SCHEMA, Siracusa.

1. Introduction

The main purpose of this work is the assessment of the tsunami-related vulnerability and losses in an urban environment by two different methods widely applied in the specialized literature (that will be denoted as SCHEMA and PTVA-3 in the paper) and the comparison of the results. The experiment is motivated by the need to assess the consistency of the methods, which will be disproven if the methods provide quite different pictures of vulnerability and losses. The target area of this study is the town of Siracusa (see Fig. 1) on the eastern coast of Sicily, Italy, a medium-size town which, according to historical records and to our present knowledge and understanding of the regional tectonic setting, is exposed to the threat of tsunamis induced by earthquakes and landslides. Siracusa, together with the neighboring town of Augusta, is one of the test sites of the FP7 project ASTARTE (Assessment, STrategy And Risk Reduction for Tsunamis in Europe, http://www.astarte-project.eu/) that aims, among other objectives, to identify strengths and weaknesses in the current methods of assessing tsunami vulnerability and risks in the European region, and that forms the general frame for the present study.

The organization of the paper is as follows. After outlining the main features of Siracusa, we provide a succinct view of the historical tsunamis and of the potential tsunami sources affecting the town. Then we delineate the SCHEMA and PTVA-3 methods. Further, we will present in detail the application of the two methods to Siracusa and finally we will compare the results and discuss the significance of similarities and differences.

2. The Town of Siracusa

Siracusa is one of the most ancient towns of Italy founded on the eastern coast of Sicily on the little island of Ortigia (about 1.6 km long and 800 m wide) by Greek colonizers from Corinth and Tenea about 734 BC. It was one of the most powerful city-states of Magna Grecia and of the Mediterranean basin.

[1] Department of Physics and Astronomy (DIFA), Sector of Geophysics, University of Bologna, viale Berti Pichat 8, 40127 Bologna, Italy. E-mail: gianluca.pagnoni3@unibo.it

Figure 1
Siracusa is located on the eastern coast of Sicily, Italy. The *small inset* shows the gulf of Siracusa and the town, whose old core is on the island of Ortigia, barring the northern side of the gulf

During the Roman republican and imperial domination, it remained an important town of the Roman world. But in the course of the history, though with alternating fortunes, Siracusa progressively lost its centrality in Sicily where it was substituted by other towns like Palermo. Today Siracusa preserves a great deal of its historic patrimony (Greek and Roman archeological remains, medieval castles, baroque churches, palaces, etc.), which constitutes a well-known cultural attraction for tourists who visit the town not only in summer season, but also during the rest of the year.

Siracusa started to expand beyond Ortigia only in the second half of the nineteenth century when the so-called Umbertin quarter and the quarter of Santa Lucia were built on the mainland just to the north of the island after the city's Spanish walls were destroyed in 1870. A second more intense urbanization process started after the end of the World War II, when most of the northern quarters were built and the town assumed the aspect we know today. According to the last Italian national census (October 2011), Siracusa counts approximately 118,000 residents with a decrement of about 6 % from the 1991 peak value. The main economic activity of Siracusa is the heavy industry that is concentrated in the coastal district north of the town, including part of the Siracusa territory as well as the municipalities of Melilli,

Augusta and Priolo Gargallo. This is the main source of permanent and temporary jobs in the province and induced part of the Siracusa population to migrate from the town to the district, which explains the aforementioned demographic decrease.

Siracusa is a marine town with a long tradition of commercial trades, that however have progressively declined in recent times due to the strong competition from the neighboring harbors of Catania and Augusta. The harbor structure of the town is formed by two ports that today have both mainly touristic vocation and are oriented to yacht and boat mooring. They are called the small harbor (Porto Piccolo) and the big harbor (Porto Grande) and are found, respectively, to the north-east and to the south of the island of Ortigia. To reverse the declining trend of harbor activities, Siracusa administrators have devised projects for the requalification of the entire port structures. These projects (Marina di Siracusa, Porto di Spero, Marina di Archimede), currently under discussion, are partly being implemented and might be fully realized in the next few years.

3. The Tsunami Threat for Siracusa

Eastern Sicily together with southern Calabria is the Italian region with the strongest tsunami activity and where the largest events of the Italian tsunami history took place according to the Italian catalogue of tsunamis (Tinti *et al.* 2004). The largest tsunamis that hit eastern Sicily in modern history are the tsunami of 11 January 1693 and the tsunami of the 28 December 1908. It is worth pointing out that the real cause of both tsunamis is still debated (see Billi *et al.* 2010), since it is still unclear if they were triggered by the earthquakes or by one or more mass failures induced by the shocks.

3.1. The 1693 Tsunami

On 11 January 1693 an $M = 7.4$ earthquake occurred following a destructive $M = 6.2$ foreshock that took place 2 days before. The earthquake hit south-eastern Sicily including the coastal provinces of Catania and Siracusa, as well as the province of Ragusa. The two earthquakes together caused large destruction and more than 50,000 fatalities (Guidoboni *et al.* 2007). Severe seismic damage was caused even in Siracusa and especially in Ortigia. The tsunami was observed with damaging effects all along the eastern Sicily coast. The largest impact was in Augusta, a few kilometers north of Siracusa, where the harbor was first completely dried by the water withdrawal and then the sea rose by about 2.5 m above the normal level and inundated the town with run-up reaching 8 m, as reported by coeval sources (see ASV 1693; Burgos 1693; Boccone 1697; Bottone 1718). In Siracusa three main tsunami waves were observed (starting with a sea recession, as in all other Sicilian sites), and the inundation was not larger than 150 m inland (Baratta 1901; Gerardi *et al.* 2008), but the information is too poor to allow one to localize precisely the place or places where the coast was flooded.

The parent fault of the 1693 main shock was located onshore by researchers who took into account only seismic data (see Sirovich and Pettenati 1999; DISS 2010), or offshore in the Ionian Sea, along the Malta escarpment (Piatanesi and Tinti 1998; Bianca *et al.* 1999; Tinti *et al.* 2001) or in the Calabria subduction zone (Gutscher *et al.* 2006), by models trying to explain the tsunami as induced directly by the earthquake. In addition, also the hypothesis of a submarine landslide triggered by the earthquake was advocated, which, introducing distinct sources for the earthquake and the tsunami, is compatible with a seismic fault placed onshore (Tinti *et al.* 2007; Argnani *et al.* 2012).

3.2. The 1908 Tsunami

The 28 December 1908 earthquake and tsunami form together the most disastrous natural event that hit Italy in modern history, and the tsunami is the last major tsunami that occurred in the Mediterranean. The $M = 7.1$ earthquake caused great devastation in eastern Sicily and southern Calabria destroying Messina and Reggio Calabria with a toll of over 80,000 people (Baratta 1910). The tsunami is the best known of the Italian catalogue, since many data and abundant documentation were collected in ad hoc field surveys through direct measurements and interviews (e.g., Platania 1909a, b) and a number of

specific contributions were published by coeval scholars and researchers (e.g., Martinelli 1909; Mercalli 1909; Baratta 1910). The tsunami attacked the coast a few minutes after the earthquake and was more severe in the southern part of the Messina Straits where run-up heights in excess of 10 m were measured on the coasts of Lazzaro and Pellaro in Calabria and at Sant'Alessio in Sicily (Platania 1909a). The run-up heights attenuated going southwards and in the region of Augusta and Siracusa they were in the order of 2 m (Platania 1909a). In Siracusa the tsunami attacked the outer jetty of the small harbor and travelled along the channel connecting the small harbor to the big harbor. The area around the channel was flooded, but the tsunami did not travel beyond the square of the Postal Palace and the archeological site of the Doric temple of Apollo, circa 100 m from the channel bank. The inhabitants believed that Siracusa was preserved from the tsunami attack thanks to the protection of Saint Lucy, the patron of the town, and in her honor, 1 year later, they erected a devotional thanksgiving aedicule in the tsunami inundation zone. Every year on the day of the anniversary of the tsunami, the population expresses gratitude to the Saint with special religious ceremonies.

The fault responsible for the 1908 earthquake is unanimously recognized to be in the Messina Straits, though there is no consensus on the detailed geometry and slip distribution and a number of models were suggested in the literature (e.g., Monaco and Tortorici 2000; Valensise and Pantosti 1992; Piatanesi *et al.* 2008; DISS Working Group 2010; Aloisi *et al.* 2013). The difficulty in reconciling the available seismic and geodetic data with tsunami data in a global inversion procedure was first pointed out by Piatanesi *et al.* 1999, and by Tinti and Armigliato 2000 and 2001. Later the hypothesis of a huge landslide as an additional source for this tsunami was proposed by Billi *et al.* (2008). Though that specific source was considered questionable and inadequate by other authors (Argnani *et al.* 2009), the idea that the 1908 tsunami has to be mostly ascribed to the effect of one or more submarine mass movements set in motion by the earthquake is considered plausible and a fruitful subject of investigation (Favalli *et al.* 2009; Ridente *et al.* 2014).

3.3. Other Tsunamis

It is not in the scope of this paper to reconstruct the full history of tsunamis that affected the area surrounding Siracusa. It is convenient, however, to add some more information, starting from the last tsunami event that occurred on 13 December 1990, when a $M = 5.6$ earthquake with epicenter off Brucoli north of Augusta, and with strike–slip focal mechanism, took place causing severe damage in several villages (Amato *et al.* 1995; Barbano *et al.* 2001). The earthquake was too small and with unfavorable focal mechanism to generate a tsunami, but some effects were anyhow produced and reported (Boschi *et al.* 1997). In Augusta, some anomalies of the ordinary sea wave pattern were observed and the littoral road called Lungomare Granatello was flooded by sea water. Some kilometers to the north, off Agnone, some seamen noticed a change in the pre-earthquake sea depth, which was suggestive of submarine slides, and smaller slides were also advocated to explain further sea depth changes off Catania. In summary, though there are no instrumental records confirming that a tsunami took place, there are a few hints that this medium-size earthquake may have destabilized the sea bottom in several places and generated a number of small tsunamis all along the coast from Augusta to Catania.

Tsunami geology can extend the records of tsunamis affecting a target coast beyond the limit of historical documents. Tsunami deposits in the form of big scattered boulders and of sediment layers were identified in several sites along the eastern coast of Sicily (Scicchitano *et al.* 2007, 2010; De Martini *et al.* 2010, 2012; Smedile *et al.* 2012) and were associated to paleo- as well as historical tsunamis. The most relevant of these are 3 local and 2 remote tsunamis. The local tsunamis are the already mentioned 1693 and 1908 tsunamis and, in addition, a tsunami that occurred in 1169 and on which information is rather poor (Tinti *et al.* 2004). The remote events are the 365 AD tsunami, due to an earthquake in the western Hellenic Arc west of Crete (see the tsunami model by Shaw *et al.* 2008 and the presumed generation of a megaturbidite in the Ionian Sea by Polonia *et al.* 2013) and the tsunami caused by the

explosion of Santorini some 1600 years BC (McCoy and Heiken 2000).

4. Tsunami Scenarios for the Town of Siracusa

Tsunami vulnerability and damage analyses require inundation maps as input since the level of damage incurred by vulnerable elements depends on the characteristics of the tsunami flow. Inundation maps can be the outcome of probabilistic tsunami hazard analyses (though most of these applications are restricted to computing the wave height at the coast; see e.g., Tinti 1991; Geist and Parson 2006; Burbridge *et al.* 2008; Brizuela *et al.* 2014) or of assessments based on credible tsunami scenarios (see Grilli *et al.* 2011; Tonini *et al.* 2011; Pagnoni *et al.* 2015).

Since our study is focused on the comparison of two different vulnerability and loss estimate methods, we opted for considering simplified reasonable inundation scenarios, that is by considering that the coast is flooded by a uniform increase of the sea level induced by the tsunami, which is usually referred to as the bath-tub hypothesis (see Eckert *et al.* 2012). Assuming a constant-level inundation implies that the main parameter involved in the vulnerability and damage computations is the tsunami flow depth, and that the velocity of the tsunami currents has no influence in producing damage on the exposed elements. This is an approximation that is usually done in this field and is mainly justified by the circumstance that very often the only data that can be obtained by post-tsunami surveys are the maximum height reached by the sea onshore, while data on water speed cannot be retrieved, if not exceptionally (see Fritz *et al.* 2012).

We will explore three tsunami scenarios for the town of Siracusa, with inundation heights of 1, 3 and 5 m. The question arises if considering these height levels is reasonable. More specifically one might wonder if assuming that Siracusa is flooded by a 5-m tsunami is a credible scenario or not. The main doubts can be derived from the observation that, from the known tsunami history of the town, tsunami heights as large as 5 m were never reported in the town. Some more doubts can be derived from the work of Sørensen *et al.* (2012) who evaluated the tsunami hazard in the whole Mediterranean. The eastern Sicily coast including Siracusa is their region 7 and the maximum expected tsunami height results do not exceed 2 m for a 500-year time span and to be in the order of 5 m for a period of 5000 years. However, there are a number of arguments that can be invoked in support of our hypothesis.

The first argument regards the local earthquake sources. The most recent databases of the Italian active faults are denoted as DISS (see Basili *et al.* 2008) and as SHARE-EDSF (Basili *et al.* 2013), the former being focused on the Italian region and the second being an update of the former and an extension to the Mediterranean area. In DISS terminology, the source areas that are best known and characterized are called individual seismogenic sources (ISS) and composite seismogenic sources (CSS), while others deserving more research are called debated seismogenic sources (DSS). It is worth pointing out that, as regards south-eastern Sicily, the two databases are perfectly coincident, and that all the sources of type ISS and CSS are located onshore and are incompatible with tsunami generation. The only source in DISS that can generate tsunamis is of the type DSS and runs offshore, parallel to the Malta escarpment from Catania to Siracusa. A similar fault was included in the catalog of the tsunamigenic sources for the European area that was assembled in the European 2006–2009 project TRANSFER (http://www.transferproject.eu/). Numerical simulations to explain the 1693 tsunami carried out by Piatanesi and Tinti (1998) and by Tinti *et al.* (2001) took into account this offshore fault and some other variants, but all assumed that the rupture did not affect the southern sector of the fault in front of Siracusa, since most of the observed tsunami effects were reported in Augusta and to the north of it. That the entire fault segment, including the southern sector, might break was assumed by Tinti *et al.* (2005a) who described possible giant tsunami scenarios in the Mediterranean, but focused on the open sea propagation and did not pay attention to the local effects on Siracusa. What we stress is that, though debatable, nobody can exclude, on the basis of the present imperfect knowledge of the regional seismotectonics, that there is an active fault off eastern Sicily running almost

parallel to the coast in correspondence with the Malta escarpment. Further, nobody can exclude that this fault is capable of earthquakes of magnitude larger than 7 and even up to 8 (see Tinti *et al.* 2005a; Sørensen *et al.* 2012) and that in the future the sector of the fault in front of Siracusa might break. If we further add that big earthquakes are almost always associated with rather heterogeneous slip distributions on the fault, we can come to the conclusion that the scenario of a big local earthquake occurrence with a patch of a large co-seismic slip off Siracusa is credible, and equally credible is that the town could be consequently inundated up to a level considerably larger than the known historical evidence of 2 m.

The second argument regards remote earthquake sources. The western Hellenic Arc going from western Crete to the Peloponnesus is a source of big earthquakes with potential for large tsunamis. The 365 AD tsunami is one example of such occurrences. It was observed in the whole eastern Mediterranean and affected also the central Mediterranean coasts, including Sicily (Guidoboni *et al.* 1994). Numerical tsunami simulations show that a large earthquake in that area generates a tsunami with most of the energy directed to the south-west against the coasts of Libya and Tunisia, with some local effects also on the coasts of eastern Sicily (Tinti *et al.* 2005a; Shaw *et al.* 2008). In addition, there is strong geological evidence that the 365 AD tsunami propagated toward the west and inundated Sicilian coasts. Recently, Polonia *et al.* (2013) reinterpreted the Homogenite, also known as Augias turbidite, that is found in the Ionian and Sirte abyssal plains as due to the effect of the 365 AD tsunami propagating westward rather than of the tsunami caused by the Santorini caldera collapse, as previously suggested by Kastens and Cita (1981) and later supported by other studies (see e.g., Cita and Rimoldi 1997). Moreover, from a number of sediment cores taken in 10 sites onshore and one site offshore along the eastern coast of Sicily, and spanning a period of about 4000 years, Smedile *et al.* (2012) were able to suggest the association of sediment layers with the 365 AD tsunami in at least 4 of the 10 onshore sites (namely, Torre degli Inglesi, Gurna, Priolo Gargallo and Morghella) as well as in the offshore site in Augusta Bay. In addition, analyzing fine-to-coarse sediment deposits in a narrow embayment at Ognina, Schicchitano *et al.* (2010) were able to attribute them to the 365 AD event. Since some of these sites are located to the north and some to the south of Siracusa, it is reasonable to assume that also Siracusa was affected by this tsunami. Further, considering that the inundation distance where the cores were taken is more than 500 m in Priolo Gargallo and beyond 1200 m in Morghella (De Martini *et al.* 2012), one can assume that the tsunami was large enough to cause extensive flooding even in Siracusa. The second argument can be summarized then as follows. Even though there are no specific tsunami accounts in the historical records concerning Siracusa, nobody can exclude that the 365 AD tsunami inundated the area surrounding Siracusa and the town itself, and, moreover, nobody can exclude that a big earthquake taking place in the western Hellenic Arc can produce inundation of several meters in Siracusa, if the fault geometry and slip distribution are favorable.

The third argument regards landslide sources. It has been already mentioned that the 1693 and the 1908 tsunamis are still subject to active research, because there is no consensus on the genetic fault for either of them and also because it has been suggested that they are the result of submarine landsliding. That the slopes of the Messina Straits and the Malta escarpment are areas prone to mass failures is known from a number of morpho-bathymetric surveys (Argnani and Bonazzi 2005; Ridente *et al.* 2014). Further, we note that even a medium earthquake like the 13 December 1990 shock was able to set in motion a number of submarine slides off Augusta and in the Gulf of Catania, as reported by fishermen (Boschi *et al.* 1997). And in addition we can mention the damage of two telegraph cables connecting Sicily and Calabria across the Straits of Messina, and the break of a long cable connecting Malta and the Greek island of Zante across the Ionian Sea after the 1908 Messina earthquake. This was taken by Ryan and Heezen (1965) as the proof that a slump was induced by the earthquake and that it evolved into a turbidity current able to travel over 120 miles and to intercept the cable. A further consideration is that local tsunamis with high run-up can be produced even by small-volume landslides. The 2002 tsunami that produced severe damage in Stromboli was shown to

have been generated by two landslides along the north-western slope of the volcano in the so-called Sciara del Fuoco, none of them having volume larger than 40 million m^3 (Tinti *et al.* 2005b; Tinti and Pagnoni 2006). And recently, Zaniboni *et al.* (2014) showed through numerical simulations that submarine landslides in the Malta escarpment with volume of 150 million m^3 are able to produce waves larger than 6 m at the Sicily coast. Taking into account all the previous considerations, the third argument is that nobody can exclude that a small-volume landslide can be triggered even by a moderate earthquake in the Malta escarpment sector off Siracusa and that the landslide can generate a tsunami able to flood the town.

On the basis of the above three arguments, we believe it is reasonable to explore inundation scenarios for Siracusa in the range of 1–5 m flooding, which however does not mean that we consider the 5-m level as the extreme inundation limit for the town. To determine the maximum level a detailed tsunami hazard analysis should be carried out, but this is outside the scope of the present paper.

5. Tsunami Vulnerability and Damage Analysis Methods

Vulnerability to tsunamis, like in general tsunami science, had a spectacular advancement in the decade after the catastrophic 2004 Boxing Day tsunami in the Indian Ocean, since it attracted the attention of many more researchers and practitioners. In spite of this, there is still a lack of systematization even of the basic concepts and terminology (see Birkmann and Fernando 2008; Camarasa Belmonte *et al.* 2011). In this paper, we restrict our attention to assess the vulnerability of buildings to the impact of tsunamis and we will apply two different methods that were developed by different groups in different frames and were both applied extensively in different regions of the world. As anticipated before, we will call them SCHEMA and PTVA-3 in this paper and we will give a succinct outline of them in the following, while for all other details the reader can refer to the original papers.

5.1. The SCHEMA Method

SCHEMA (Scenarios for tsunami Hazard-induced Emergencies Management) is the acronym of a European FP6 project. One of its goals was the development of a new method for tsunami vulnerability assessment. In SCHEMA, vulnerability analysis covered all the possible elements or assets: inanimate static objects (like buildings, bridges, infrastructures), inanimate mobile objects (like cars, trains, buses, boats), animate entities (like persons), etc. But most of the efforts were devoted to cover buildings vulnerability and damage evaluation. Primary and secondary factors were recognized to influence the capability of a building to resist tsunami attack. Primary factors deal with the intrinsic properties of the building, that is construction materials and structure, including foundation. Secondary factors have mainly to do with the physical context, including ground type, building orientation, distance from shoreline, existence of possible direct or indirect protections (like walls), vicinity to floating debris sources (e.g., marinas, open-air parking places), etc. A third group of factors has to do with the hydrodynamic characteristics of tsunami waves, such as flow depth, flow speed and drag, number and period of waves, etc.

In the SCHEMA project, a building classification scheme was set up according to the primary factors of vulnerability. It was built using a work by Leone *et al.* (2010) who analyzed the damage to constructions caused in Banda Aceh, northern Sumatra, by the Indian Ocean tsunami, but was modified to adapt it to European building standards (Valencia *et al.* 2011). It was further assumed that the main flow feature influencing damage is the flow depth, also known as the height of the water column, and, for each building class, a damage function was built on the basis of experimental data. The damage function provides the maximum level of damage that a building may incur corresponding to a given maximum flow depth (Gardi *et al.* 2011; Valencia *et al.* 2011). In this paper, we use the SCHEMA classification that is given in Table 1: building classes go from class A (light constructions) to class E (reinforced concrete buildings). The damage to buildings is in turn discretized in 6 levels going from D0 (no damage)

Table 1

Building classes depending on the resistance characteristics of the constructions after the SCHEMA project

Class	Building types	Number of floors
I. Light constructions		
A	Beach or sea-front light constructions/shanty town/old town. Wooden, timber, clay materials, slabs of zinc	1
II. Masonry constructions and not reinforced-concrete		
B	Bricks not reinforced, cement mortar wall, fieldstone, masonry	1
C	Individual buildings, villas, hangars	1 or 2
	Bricks with reinforced column and masonry filling	
D	Large villas or collective buildings, residential, commercial or industrial buildings. Concrete not reinforced	Any
III. Reinforced-concrete constructions		
E	Residential or collective structures or offices, car parks, commercial or industrial buildings	Any
	Reinforced concrete, steel frames	

to D5 (total collapse). The damage discretization implies a corresponding discretization of the damage functions that in SCHEMA are represented altogether by means of a damage matrix. The matrix we use in this work is given in Table 2. Each building class corresponds to a matrix column. Classes are ordered from A to E, that is in decreasing level of vulnerability. Vice versa, the rows are ordered for increasing level of damage from D1 to D5. Notice that level D0 is missing since it is assumed that a building has no damage if it is not reached by the tsunami, that is if the maximum flow depth is zero. In the columns, one can read the flow depth intervals producing a specific level of damage. The flow depth values are expectedly increasing with the damage level. It is worth mentioning that the SCHEMA method was applied in a number of test sites, namely in Setúbal, Portugal (Ribeiro *et al.* 2011), in Rabat, Morocco (Atillah *et al.* 2011), as well as in Mandelieu, close to Nice, France, and in Balchik, Bulgaria (Tinti *et al.* 2011) and in Alexandria, Egypt (Pagnoni *et al.* 2015). The application of the SCHEMA method to the Italian site of Catania, eastern Sicily, deserves special mention, since Catania is located not far from Siracusa (see Tinti *et al.* 2010).

5.2. The PTVA-3 Method

By PTVA, an acronym standing for Papathoma Tsunami Vulnerability Assessment, one denotes a method to evaluate vulnerability that was first devised by the Greek researcher Papathoma who applied it to the Cretan town of Heraklion (Papathoma *et al.* 2003). This followed a previous attempt to study consequences of a tsunami in Heraklion made by Papadopoulos and Dermetzopoulos (1998) and,

Table 2

Damage matrix obtained by discretizing the SCHEMA damage functions and modified after Reese et al. (2007)

Damage level	A	B	C	D	E
Light damage					
D1	0–0.5	0–1	0–2	0–2.8	0–3
Important damage					
D2	0.5–1	1–2	2–4	2.8–4.5	3–6
Heavy damage					
D3	1–2	2–4	4–6	4.5-6.5	6–9.5
Partial collapse					
D4	2–3	4–5	6–8	6.5–9	9.5–12.5
Total collapse					
D5	>3	>5	>8	>9	>12.5

Inundation depths are in meters. The letters (A, B,…,E) in the first row indicate the SCHEMA vulnerability class

together, constitute the first examples of a vulnerability and damage evaluation carried out in Europe before the 2004 Indian Ocean tsunami. The method was further applied to Akoli and Selianitika, two small coastal villages in the Corinth Gulf, Greece (Papathoma and Dominey-Howes 2003), and later validated on the Maldives that were attacked by the Indian Ocean tsunami (Dominey-Howes and Papathoma 2007).

We will use here a revised version of the method, that is also known as PTVA-3 (Dall'Osso *et al.* 2009a), that was used to evaluate buildings vulnerability in Sidney, Australia (Dall'Osso *et al.* 2009b) and later validated in Stromboli, Italy, after the damaging tsunami of 30 December 2002 (Dall'Osso *et al.* 2010). In PTVA-3 the vulnerability of a building (Bv) is an integer index ranging from 1 to 5. In order to compute it, PTVA-3 introduces first an intermediate index, Bv' that is computed by taking into account as many as $N = 7$ structural parameters or attributes that are listed in Table 3. Each attribute is graded by a score P_k ($k = 1,2,\ldots N$) selected by the evaluator among the options proposed in the table. The index Bv' is the weighted average of these scores where the weights W_k are appropriate numerical constants that were calibrated in the field (Dall'Osso *et al.* 2009a):

$$Bv' = \left(\sum_{k=1}^{N} P_k W_k\right) \Big/ \sum_{k=1}^{N} W_k \qquad (1)$$

In the original PTVA-3 notation, buildings attributes are P_1 the number of stories (s), P_2 the type of construction material (m), P_3 the degree of the ground floor openness (g), P_4 the type of foundation (f), P_5 the shape and orientation (so), P_6 the presence of movable objects (mo), and P_7 the preservation conditions (pc). By construction, the index Bv' can take values within the interval $[-1, +1]$ and is linearly mapped and discretized in the integer index Bv with five levels from 1 to 5.

In order to assess the damage incurring to a building, the PTVA-3 method introduces two more indices designated by $Prot$ and Ex called, respectively, protection and exposure. Following the previous procedure, an intermediate index $Prot'$ is computed according to Table 4 in a way similar to the one used for the index Bv', that is as a weighted average of $N = 4$ parameters. In this case, the parameters are P_1 the number of building rows interposed between the shoreline and the building itself (br), P_2 the presence of natural barriers (nb), P_3 the height and shape of seawalls (sw), and P_4 the height of possible walls around the building (w). Like for Bv', the index $Prot'$ is also scaled from its original range [0,1] to the interval [1, 5] and transformed into the five-degree index $Prot$. Eventually, the exposure Ex is also an integer index ranging from 1 to 5. It is 5 if the maximum flow depth at the building is larger than 4 m, while in all other cases Ex is simply the maximum flow depth expressed in meters and rounded to the next upper integer.

The following step of the PTVA-3 method is the computation of the structural vulnerability index Sv, that is an integer index going from 1 to 5. It is obtained through the intermediate index Sv' that is

Table 3

Attributes to compute the intermediate vulnerability of a building Bv' according to the PTVA-3 method

Attribute	−1	−0.5	0	+0.25	+0.5	+0.75	+1
s (number of stories)	> 5	4	3		2		1
m (material)	Reinforced concrete		Double brick		Single brick		Timber
g (ground floor hydrodynamics)	100 % open plan	75 % open plan	50 % open plan		25 % open plan		Not open plan
f (foundation strength)	Deep pile		Average depth				Shallow
so (shape and orientation)	High		Average				Poor
mo (movable objects)			Minimum	Moderate	Average	High	Extreme
pc (preservation condition)	Excellent	Good	Average		Poor		Very poor

Table 4

Attributes to compute the intermediate protection level of a building Prot′ according to the PTVA-3 method

Attribute	0	0.25	0.5	0.75	1
br (building row)	>10th	7th–10th	4th–6th	2nd–3rd	1st
nb (natural barriers)	Very high protection	High protection	Average protection	Moderate protection	No protection
sw (seawall shape and height)	Vertical and more than 5 m	Vertical and between 3 and 5 m	Vertical and between 1.5 and 3 m	Vertical and less than 1.5 OR sloped and more than 1.5 m	No seawall OR sloped and less than 1.5 m
w (brick wall around the building)	Wall height more than 80 % of the water depth	Wall height between 60 and 80 % of the water depth	Wall height between 40 and 60 % of the water depth	Wall height between 20 and 40 % of the water depth	Wall height less than 20 % of the water depth

defined as the product of the indices introduced before, i.e.:

$$Sv' = Bv \times Prot \times Ex \quad (2)$$

and that therefore is an integer belonging to the interval [1,125]. This in turn can be converted to Sv by dividing Sv' by 25 and by making a proper discretization.

A further integer index going from 1 to 5 is the vulnerability due to water intrusion Wv, that is computed as the ratio between the number of inundated levels and the total number of stories of the building, multiplied by 5 and then rounded to the next upper integer.

The final index of the PTVA-3 method is the relative vulnerability index Rv that is obtained as a linear combination of Sv and Wv through the expression:

$$Rv = 2/3\ Sv + 1/3\ Wv \quad (3)$$

and that is a real number falling in the interval [1, 5]. The PTVA-3 method assumes that the index Rv is directly related to the damage level incurring to the building according to a linear relationship, that is: the damage is "minor", if $1 \leq Rv < 1.8$; it is "moderate", if $1.8 \leq Rv < 2.6$; it is "average", if $2.6 \leq Rv < 3.4$; it is "high", if $3.4 \leq Rv < 4.2$; it is "very high", if $4.2 \leq Rv \leq 5$.

In the following, it will be convenient to replace this 5-degree PTVA-3 damage scale with a quantitative scale ranging from 1 to 5. We will call it the PTVA-3 damage or simply PD scale: with "minor" corresponding to PD = 1, "moderate" to PD = 2, etc.

6. Data Sets

The data that have been used to carry out the comparative analysis of buildings vulnerability and damage are (1) technical local maps at scale 1:2000 in numerical form resulting from aerial photogrammetic surveys carried out between August 2004 and June 2005; (2) Digitalglobe satellite imagery taken in November 2011, made available by Google through Google Earth; (3) digital pictures at ground level visible through the Google Maps Street View technology, covering the whole town of Siracusa and acquired in March 2009, February and October 2010, and mostly in July 2012 and (4) data gathered through a field survey carried out by Dr. Gianluca Pagnoni and Dr. Francesco Rallo in February 2014 with the double purpose of data verification and data integration.

6.1. The CTN GIS-Oriented Maps

Since Google Earth and Google Maps products are very well known and widely used, there is no need for any specific description; however, it is convenient to better clarify the data available at the 1:2000 scale. The local maps known with the acronym CTN from the Italian denomination "Carta Tecnica Numerica" are 1:2000 sheets that are part of a cartographic map series that is published by the Regione Sicilia and covers the whole territory of Sicily. Each CTN sheet spans an interval of 1 arc prime in longitude and of 36 arc seconds in latitude.

The four sheets including the area of interest for our analysis are represented in Fig. 2. Sheets 18 and 23 cover the old town on the island of Ortigia and the Umbertin quarter bridging the island with the mainland. Sheet 13 covers the quarter of Santa Lucia and the modern town in the east, while sheet 17 covers the commercial and industrial quarters in the west. The reference frame is the Gauss–Boaga coordinate system centered on the 15°E meridian.

It is convenient to stress that CTN sheets are GIS-oriented databases, whose content is quite rich of valuable territorial, geographically referenced, information. Data are organized in thematic layers that are identified by capital letters such as A, B, C,

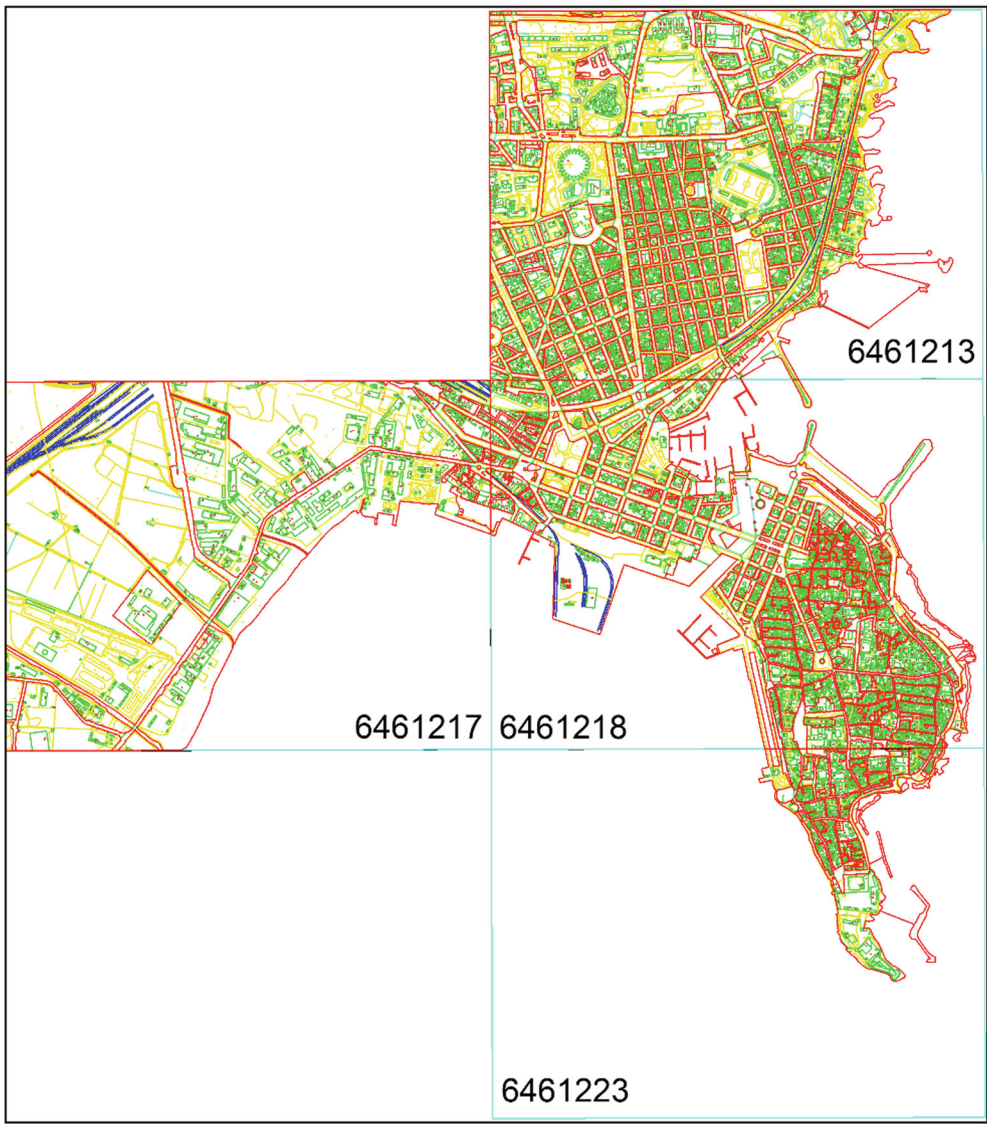

Figure 2
Union view of the four 1:2000 digital thematic charts used in this work. *Numbers* are the codes identifying the individual charts in the Sicilian map series. It is seen that sheet 6,461,213 covers the northern quarters of the town, sheets 6,461,218 and 6,461,223 cover the old historical town on Ortigia and the quarters developed between the end of the nineteenth century and the beginning of the twentieth century, while sheet 6,461,217 covers the western part of the town including mostly industrial and commercial constructions. In the paper, sheets will be identified by the last two digits of the code

etc. They are listed in Table 5 where one can find the general description as well as examples of objects or entities that are classed in each layer. The most interesting layer for the present study is layer B including data on buildings. Here it is worth observing that, for all constructions, the database contains the attribute called "elevation", giving the space-average altitude of the entity above the mean sea level taken at the ground level. This makes it very easy to select entities falling in the inundation areas, that is areas flooded as a result of an assumed sea level increase by 1, 3 and 5 m. It has to be noted that when the building lies on a slope and therefore its elevation changes over its basal area, taking the average value as characteristic for the whole building introduces some approximation error; that, however, is not crucial for the present analysis. Figure 3 provides an exemplary geographic picture of all layer B entities that belong to sheet 18 and that are at an altitude level less than, or equal to, 5 m asl.

7. Buildings Vulnerability Analysis

The analysis of vulnerability for buildings has been carried out according to the two models, SCHEMA and PTVA-3, described synthetically in the previous sections. The first step is the creation of a buildings inventory, which was done starting from the CTN data mostly contained in layer B, but also in layer C. The final result is summarized in Table 6, where one can find the layer categories and their description in the first two columns, as well as the number of entities selected for the inventory from each category (last column), under the assumption of a 5-m tsunami inundation. For a 5-m inundation, a total of 2446 buildings (entities) were inventoried. Their distribution in the town can be seen in Fig. 4, where they are also shown for different inundation levels. It turns out that only 57 constructions fall within the 1-m inundation area, with the number growing to 1161 for the 3-m level and to 2446 for the 5-m level.

Table 5

Layers of the standard 1:2000 CTN sheet

Polyline layer	General description	Examples of entities
A	Street, railway and other communication network	High-capacity way such as a highway, state road, driveway, carriageway, byway, railway, train station, lighthouse, harbor dock, jetty, aerial tramway, etc.
B	Buildings and building complexes	Residential building, industrial building, commercial building, shopping mole, sports venue, cultural center, tower, chimney, kiosk, under construction building, etc.
C	Water streams and separation border between land and waters	Sea coastline, channel bank, river bank, jetty and breakwater profile, dock profile, river, watercourse, aqueduct, lake, pond, swimming pool, water sink, water source, water fall, etc.
D	Structures connected to production and transportation of energy and data	Oil well, methane well, gathering-transportation oil and gas pipeline, excavation quarry, electric power transmission line, telecommunication line, telecommunication antenna, pump station, etc.
E	Separation and support elements	Hedgerow, fence, palisade, barbed wire fence, wall fence, wood fence, city wall, bastion, etc.
F	Morphological elements	Scarp, escarpment, detachment niche, levee, embankment, cave, natural sink, drainage basin, watershed, reef, etc.
G	Vegetation elements	Forest, wood, isolated tree, park, garden, garden center, plant nursery, vineyard, grove, olive grove, citrus grove, grove of reeds, etc.
H	Orography	Altitude isoline, aerophotogrammatic altitude at the ground
I	Administrative boundaries and other elements	Municipality border, province border, military area border, cemetery cross, etc.
L	Toponyms	Urban inhabited settlement, inhabited nucleus, scattered houses, monument, church, relevant historical building, watercourse, mountain, valley, mountain pass, plain, plateau, lowland, beach, littoral, etc.
M	Framing points	IGM trigonometric vertex, benchmark point, etc.

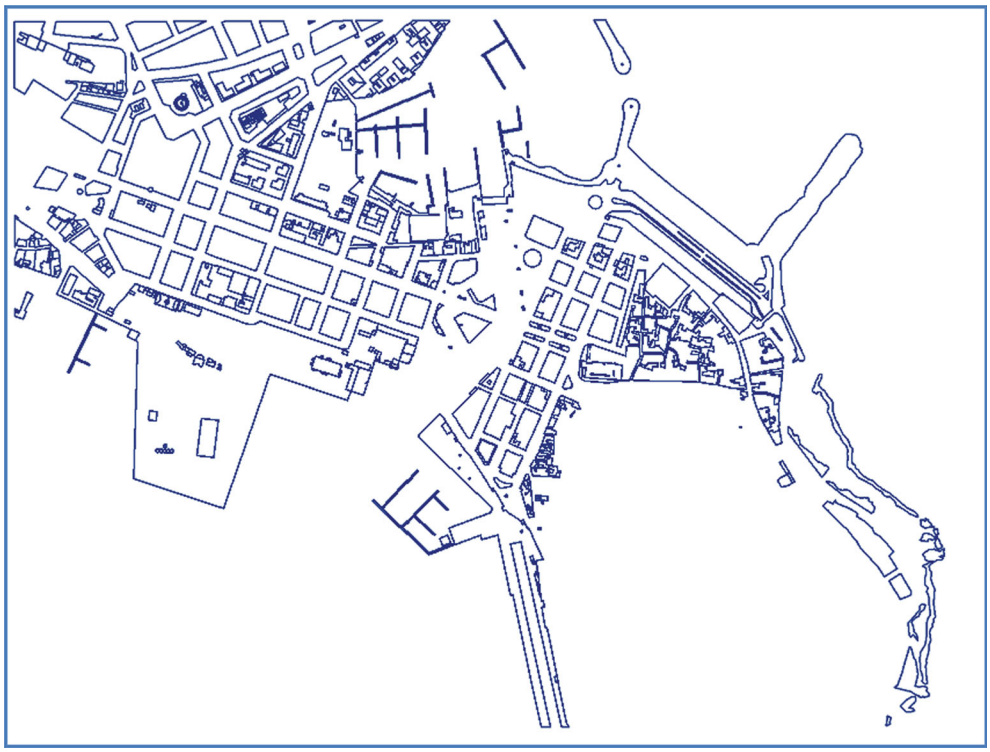

Figure 3
Sheet No. 18. Entities of layer B (buildings) with elevation less than, or equal to, 5 m

Table 6

Frequency of entities for each category (Bxxx, Cxxx) of layers B and C classified for vulnerability analysis. Only entities with altitude less than, or equal to, 5 m are counted

Category	Description	No inventoried buildings
B001	Residential building unit, service building unit, administrative building unit	1871
B002	Industrial building unit, commercial building unit, hangar, warehouse	174
B003	Religious unit, bell tower, tabernacle	7
B004	Building under construction	1
B005	Ruins	10
B006	Bar, kiosk	162
B007	Canopy, shelter	161
B009	Electric power house, electrical substations	13
B010	Stable greenhouse	2
B021	Tower, chimney, tower silo	6
C009	Artifact of aqueduct (water tower)	39
Total		2446

7.1. SCHEMA

The attribution of the inventoried buildings to classes from A to E following the scheme of Table 1 can be performed building by building. However, we have assumed that the very detailed categorization made within the CTN program could be exploited by suitably mapping the relevant categories of the CTN

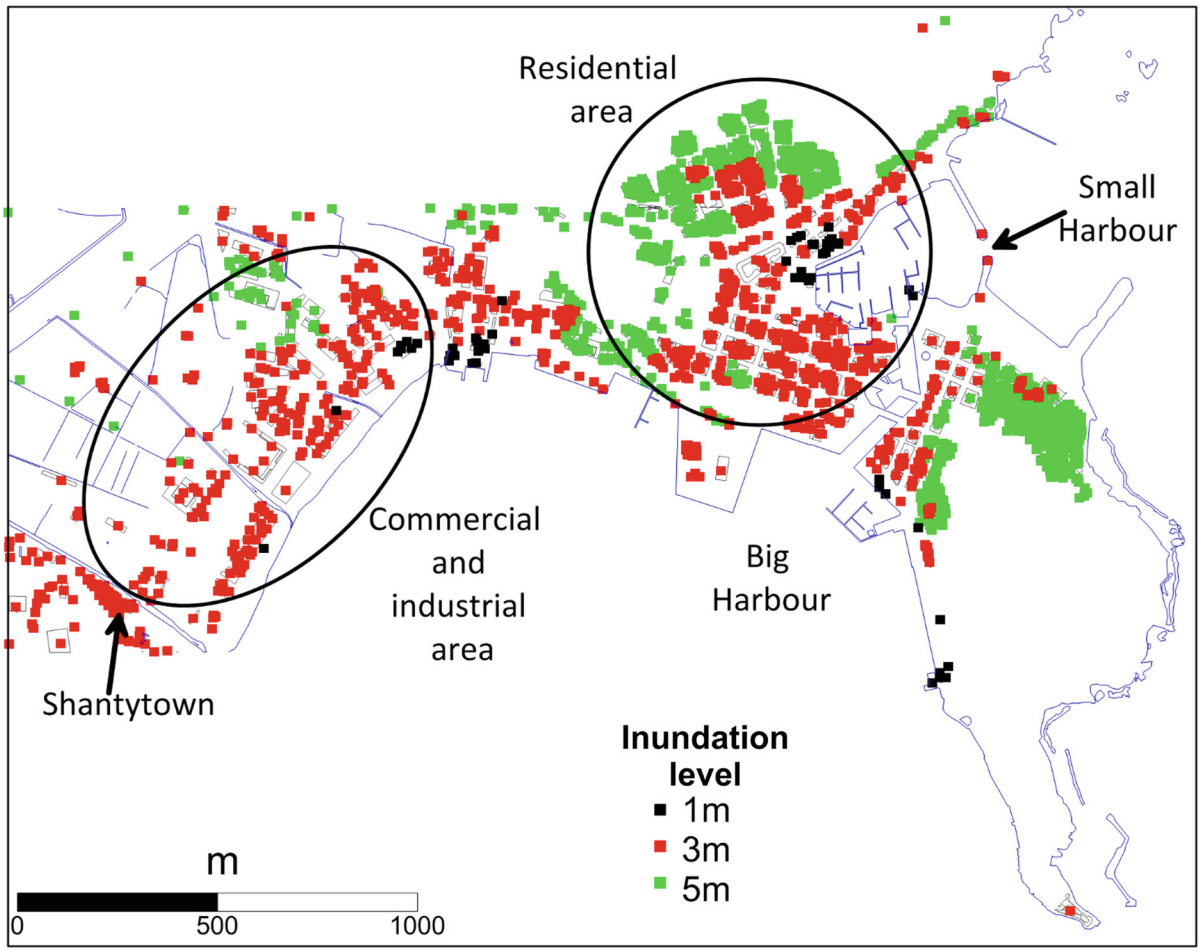

Figure 4
Inventoried buildings within the inundation areas for an assumed sea level increase of 1 m (*black*), of 3 m (*black* + *red*) and of 5 m (*black* + *red* + *green*). In the 1-m inundation area one counts 57 entities. In the 3-m one, entities are 1161, and in the 5-m one, they are 2446

layer B and C to the five classes of the SCHEMA model, and by further testing the hypothesis by direct verification (through Google Maps Street View and/or field survey). This procedure provided a satisfactory preliminary classification, that was later refined when anomalies were found. Table 7 shows the final result of the SCHEMA classification for each CTN category. It is found that several categories map into a single class (B009, B010, B021, C009), others correspond predominantly, but not exclusively, to a unique class (e.g., B001, B002, B003…), and one (B006) is mostly distributed into two classes. Most of buildings belong to category B001 and have medium-to-high resistance to tsunami impact (from class C to E). Notice further that the majority of the most vulnerable constructions (class A) belongs to categories B006 (kiosk) and B007 (canopy, shelter). Notice further that, when edifices are attached to one another in a unique house agglomerate, they have been attributed the same class, since distinction was not possible and probably could be done only at the cost of a very specific geotechnical and structural analysis. Figures 5 and 6 give pictures from the Google Earth database, showing, respectively, a typical hangar of the industrial-commercial zone in category B002 and a residential building (close to the small harbor) in category B001. Their respective SCHEMA classes are C and D. Figure 7 shows the

map of the SCHEMA-classed buildings for the 5-m inundation level. It appears that most of the buildings are in class C and are located between Ortigia and the Umbertin quarter. Further, the majority of the most vulnerable constructions (class A) are found in the west, in an area called Pantanelli, a shanty town that was built on the bank of a flood-control channel connected to the nearby stream Pisimotta.

Table 7

Number of inventoried buildings per SCHEMA classes and per relevant CTN categories, under the assumption of a 5-m tsunami inundation

Category	A	B	C	D	E	Total
B001	6	72	1604	60	129	1871
B002	1	0	173	0	0	174
B003	0	1	4	1	1	7
B004	0	0	1	0	0	1
B005	0	1	9	0	0	10
B006	93	69	0	0	0	162
B007	139	19	3	0	0	161
B009	0	13	0	0	0	13
B010	2	0	0	0	0	2
B021	0	0	6	0	0	6
C009	0	0	39	0	0	39
Total	241	175	1839	61	130	2446

The letters (A, B,…, E) in the first row indicate the SCHEMA vulnerability class

Figure 5
Picture of a typical hangar (*red circle*) in the industrial-commercial zone. Hangars are often 1-story constructions, open on at least one side, with bearing structure in iron or reinforced concrete and brick walls. Sometimes walls are replaced by large glass window. This hangar is classed in C according to SCHEMA. The PTVA-3 index *Bv* results to be 4

Figure 6
Picture of a residential building (*red circle*) that is found close to the small harbor. It is placed in the SCHEMA class D. The PTVA-3 index *Bv* results to be 3

7.2. PTVA-3

The vulnerability analysis for the method PTVA-3 ends with the determination of the building vulnerability index *Bv*. This is based on associating a set of 7 attributes (see Table 3) to each building. Most of these, *s* (number of stories), *m* (material), *g* (hydrodynamics of the ground floor), *pc* (preservation conditions) and *so* (shape and orientation) can be obtained from inspecting images and pictures, available in Google Street View. The evaluation was made case by case. As regards the foundation depth (*f*), evaluations were mostly based on the CTN categories. Categories like B006 (kiosk) and B007 (canopy) were assumed to have no foundation ($f = 1$). The same assumption was made for most of hangars in category B002, and also for all buildings on the island of Ortigia, where constructions are built on rocks and are unbolted (according to reports from local people gathered during the field survey). The value $f = -1$ (deep foundation) was instead attributed to modern buildings with three or more stories. As for the attribute *mo* (movable objects), we have graded it from minimum to extreme (see Table 3), depending on the recognizable presence of potential debris sources and on their distance. Extreme values have been attributed to buildings close to marinas and parking places. Detailed examples of evaluation are given by means of the pictures of Figs. 5 and 6. More specifically, for the hangar of Fig. 5, the attributes to compute the intermediate index Bv' are given the value *s* (1), *m* (0), *g* (0.5), *f* (1), *so* (1), *mo* (0.25) and *pc* (0) (see Table 3), which leads to $Bv' = 0.59$ and eventually to $Bv = 4$. As for the residential building shown in Fig. 6, the Bv' attributes have the value *s* (0.5), *m* (−1), *g* (0), *f* (0), *so* (1), *mo* (0.5) and *pc* (−0.5) (see Table 3), which leads to $Bv' = 0.08$ and eventually to $Bv = 3$.

Table 8 gives the results of the building classification per CTN categories. Notice that most buildings have $Bv = 4$ and none $Bv = 1$. Notice further that none of the CTN categories corresponds to a single *Bv* value (apart from B004 having only one element), and that they are distributed on several *Bv* values, though one is generally by far predominant. Only

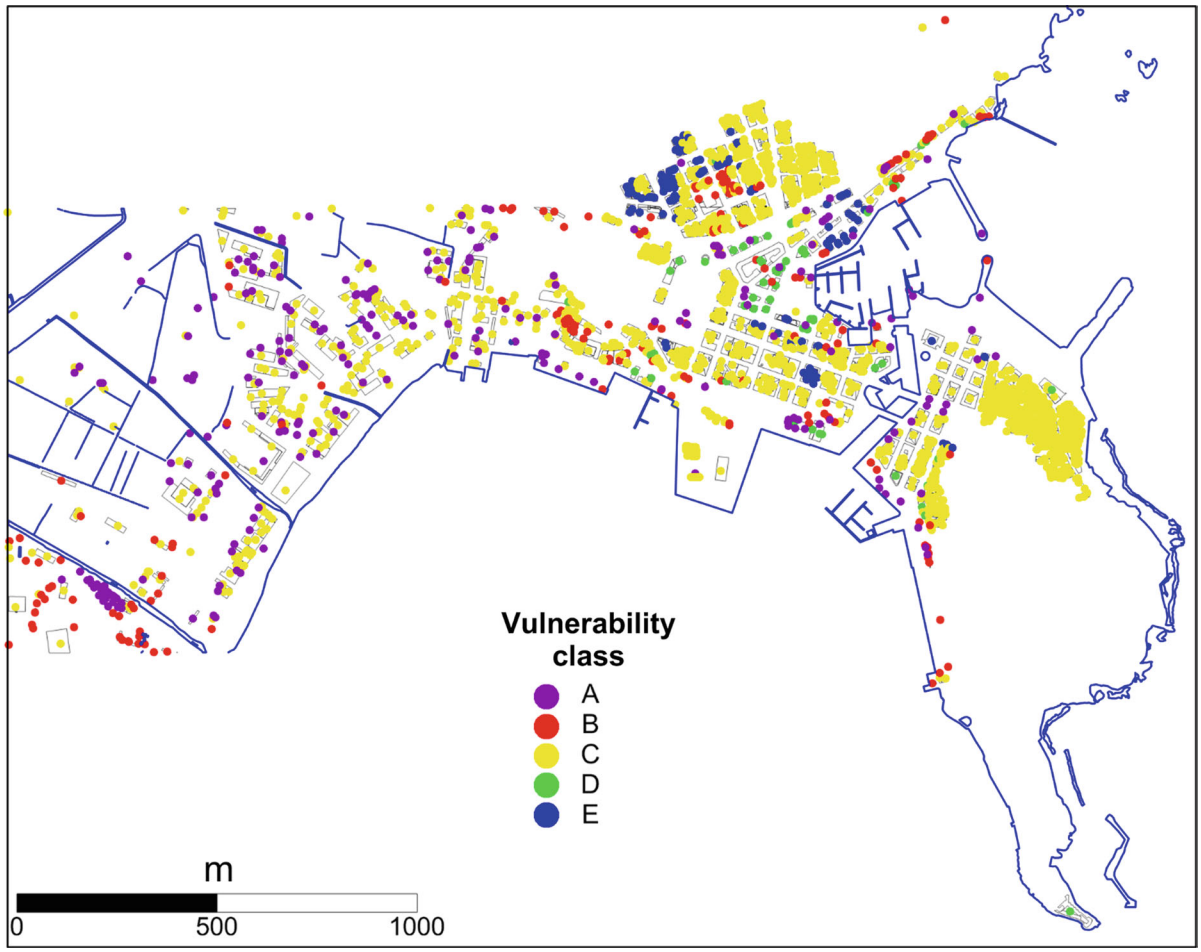

Figure 7
Vulnerability classification of buildings in the 5-m inundation area according to the SCHEMA model. Classes from *A* to *E* are in decreasing order of vulnerability

category B007 distributes more equally between $Bv = 5$ and 4. Looking at the map of Fig. 8, where the *Bv* distribution is portrayed by using the same 5-color palette used for representing the SCHEMA model, one can see that the most vulnerable structures are found close to the sea, and in the shanty town of Pantanelli.

7.3. SCHEMA vs. PTVA-3

In principle, SCHEMA classes and building vulnerability *Bv* take into account different factors and elements to evaluate the vulnerability of buildings to tsunami impact. SCHEMA model classification is more based on structural and material elements of the constructions. Instead, PTVA-3 model also accounts for environmental elements like *so* (shape and orientation), where orientation refers to the expected provenance direction of the tsunami front, and *mo* (movable objects) where proximity and intensity of debris sources are considered. Nonetheless, since both models give vulnerability graded in five discrete levels, it is of interest to put side by side the results of the vulnerability classification for comparison. Indeed, since no buildings are given $Bv = 1$, the 5 SCHEMA classes map into 4 PTVA-3 groups. Comparison is done in Table 9, from which one can see that there is a rough correspondence

Table 8

Number of inventoried buildings per different values of the PTVA-3 index Bv and per relevant CTN categories, in case of a 5-m flooding tsunami

Code	5	4	3	2	1	Total
B001	95	1541	132	103	0	1871
B002	27	147	0	0	0	174
B003	1	4	1	1	0	7
B004	0	1	0	0	0	1
B005	3	7	0	0	0	10
B006	159	3	0	0	0	162
B007	89	72	0	0	0	161
B009	6	7	0	0	0	13
B010	2	0	0	0	0	2
B021	0	6	0	0	0	6
C009	0	39	0	0	0	39
Total	382	1827	133	104	0	2446

The numbers (5, 4,…,1) in the first row indicate building vulnerability index (*Bv*) provided by PTVA-3 method

between class C and $Bv = 4$ and between class E and $Bv = 2$. Class D is more distributed between $Bv = 3$ and 4. Finally, classes A and B can together correspond to $Bv = 1$ and 2.

8. Buildings Damage Analysis

The evaluation of the damage incurring to a building as the consequence of a tsunami attack is the main topic of this section, where both models, SCHEMA and PTVA-3, will be applied and compared.

8.1. SCHEMA

The application of the damage analysis in the SCHEMA model is straightforward, once the step of the buildings classification is carried out, which indeed is the most time-consuming phase of the model. The analysis is simply done by applying the damage matrix given in Table 2: taking as input the local flooding depth and the class of a building, the matrix provides the maximum expected damage Dx on a scale from D1 to D5. The no-damage level D0 is assigned to all buildings outside the inundation area. In our case, under the hypothesis of a bath-tub tsunami inundation, the flooding depth also known as water column height is a parameter easy to compute. It is simply the difference between the assumed sea level and the asl topographic altitude of the building taken at the ground, i.e., the "elevation" which is one of the attributes of all entities, including buildings, reported in the CTN database. Results are given in the map of Fig. 9 for a supposed 5-m inundation level. It is seen that most buildings are in the damage levels D1–D2 meaning damage between light and important, that a higher damage (D3–D4) is evaluated for constructions located in lower areas close to the sea, and that total collapse (D5) is restricted to elements one finds in the shanty area of Pantanelli. A further observation is that damage levels seem to be clustered, with level D1 prevailing in Ortigia and in the Santa Lucia quarter, level D2 prevailing in the Umbertin quarters and along the coast of the western side of the bay.

8.2. PTVA-3

For the PTVA-3 model, the evaluation of the damage is as time-consuming as the buildings vulnerability analysis, since for each construction, one has to make an evaluation concerning the indices *Prot* (protection) (see Table 4) and *Ex* (exposure) to obtain the structural vulnerability index *Sv*. This index, in turn, is combined with the wave intrusion *Wv* to get the relative vulnerability index *Rv*. Eventually this converts linearly to the PD index

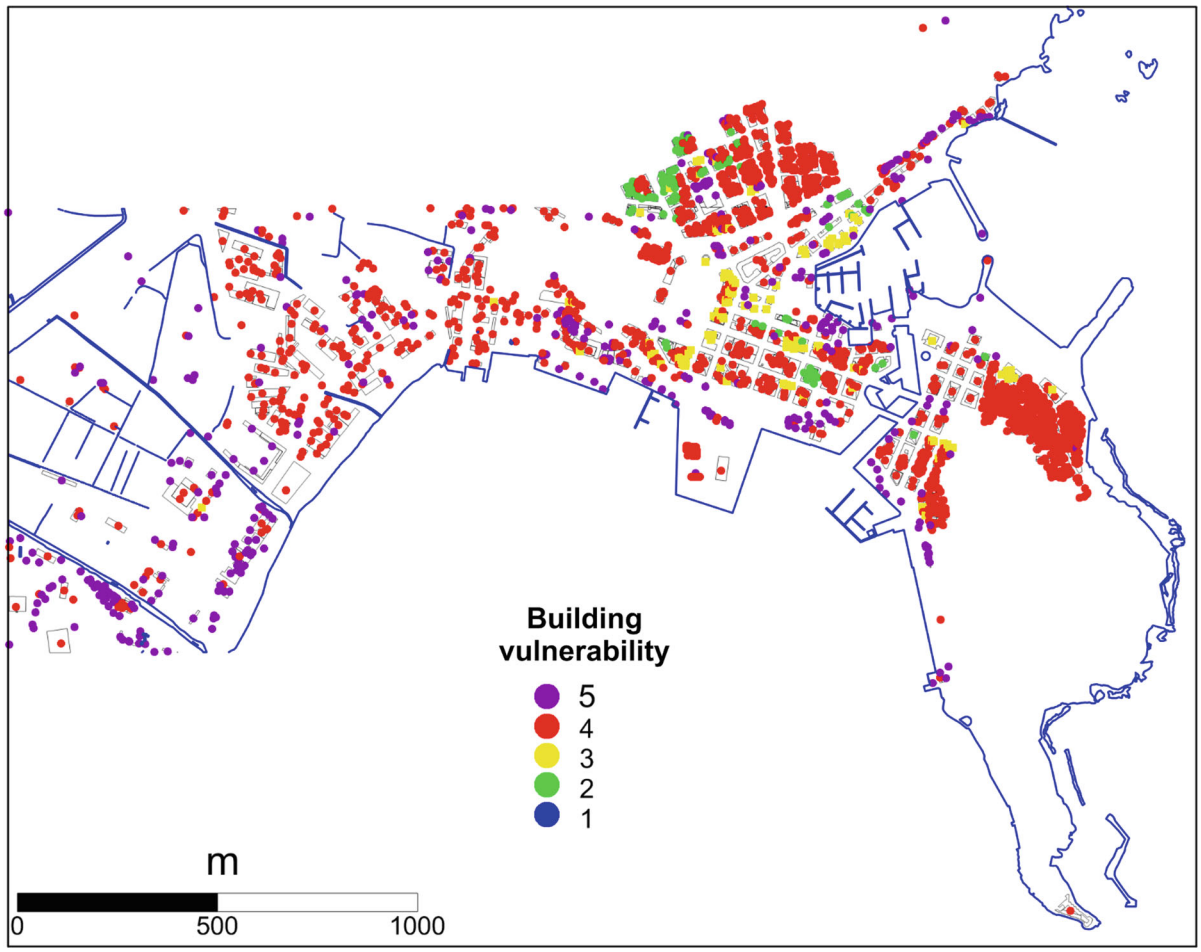

Figure 8
Building vulnerability index *Bv* according to the PTVA-3 model. Index values from 1 to 5 denote an increasing vulnerability. To favor comparison, color palette is the same used in Fig. 7 for the SCHEMA model map

Table 9

Buildings classification of SCHEMA classes vs. PTVA-3 building vulnerability index Bv

SCHEMA	A	%	B	%	C	%	D	%	E	%	Total
PTVA-3											
5	176	73	128	73	78	4.2	0	0,0	0	0	382
4	65	27	47	27	1681	91.4	34	56	0	0	1827
3	0	0	0	0	79	4.3	24	39	30	23	133
2	0	0	0	0	1	0.1	3	5	100	77	104
1	0	0	0	0	0	0	0	0	0	0	0
Total	241		175		1839		61		130		2446

The letters (A, B,…,E) in the first row indicate the SCHEMA vulnerability class, while the numbers (5, 4,…,1) in the first column denote building vulnerability index (*Bv*) of the PTVA-3 method

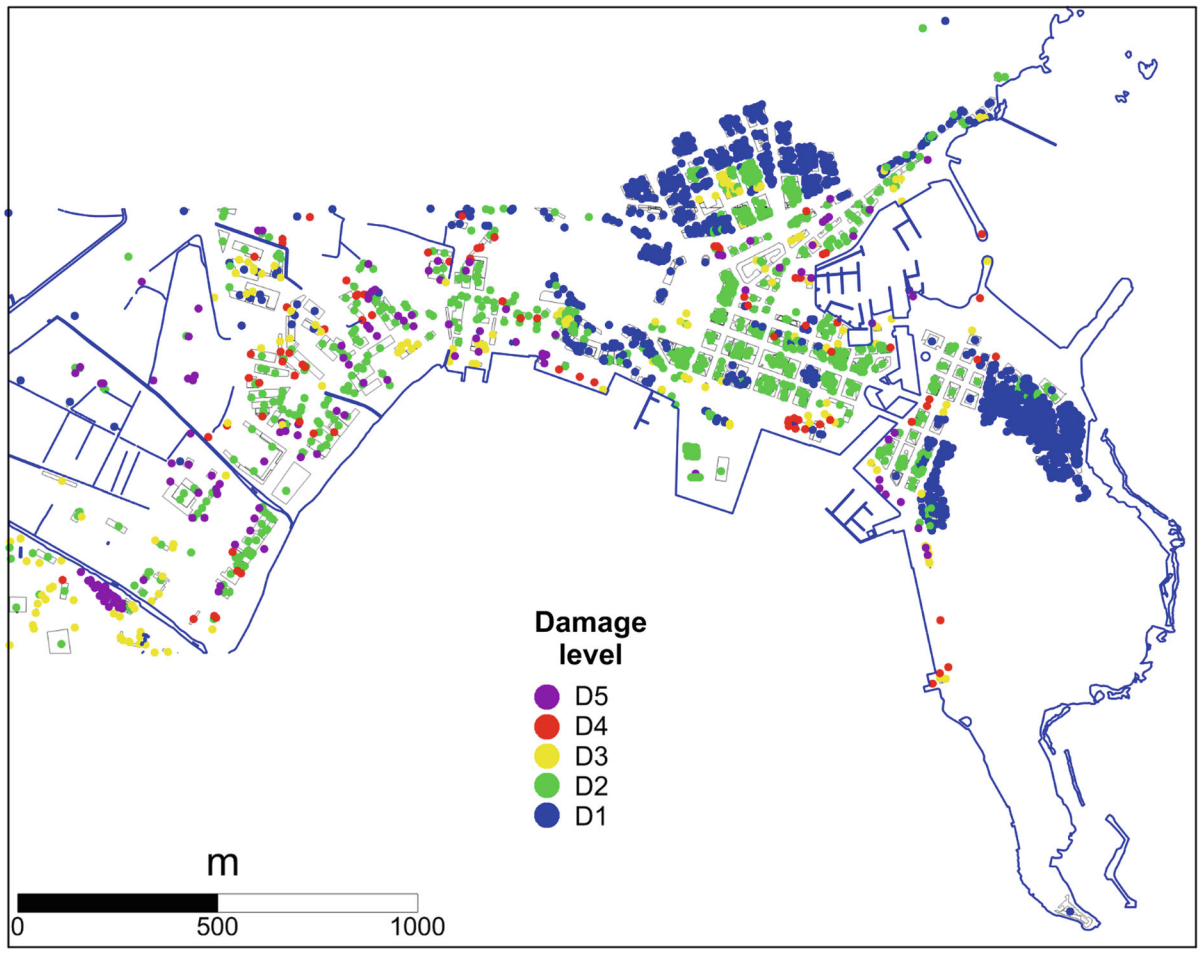

Figure 9
Damage level (Dx) of buildings for a 5-m inundation calculated via the SCHEMA model where *D1* is light damage and *D5* is total collapse

providing the expected damage level. The inundation depth enters in the computation since it influences the values of *Ex* and *Wv* as well as *Prot*, through the attribute *w* (see Table 4). Other relevant factors are the properties of the construction itself and of the surrounding environment. All involved attributes were evaluated by means of the CTN data and of Google Earth images, integrated, when needed, by the field survey. It is worth mentioning that the attribute *w* (height of possible walls around the building) needed to compute *Prot* (see Table 4) is a quantitative datum one gets very often from CTN sheets. When it was not available, it was estimated from images, which is satisfactory since only rough estimates are required by the model. Examples of index estimations are given through Figs. 5 and 6. For the hangar of Fig. 5, the four attributes to compute the intermediate index $Prot'$ are given the value *br* (1), *nb* (0.5), sw (1), *w* (0.5) (see Table 4), which implies that $Prot' = 0.79$ and eventually $Prot = 4$. For the building of Fig. 6, the $Prot'$ attributes are *br* (0.75), *nb* (0.75), *sw* (0.5), *w* (1) (see Table 4), and this implies that $Prot' = 0.74$ and eventually $Prot = 4$. Results are given in the map portrayed in Fig. 10 where the damage is shown for all buildings within the 5-m inundation area. By inspection, it is seen that the most frequent levels are "minor" (PD = 1) and "moderate" (PD = 2). The level "average" (PD = 3) is frequent in the Umbertin quarter, and above all in the industrial-commercial

area inland. "High" (PD = 4) and "very high" damage (PD = 5) are estimated not only in the shanty town area, but also for most constructions in the water front of the western coast.

8.3. SCHEMA vs. PTVA-3

The damage levels to buildings Dx and PD are the final results of the respective models SCHEMA and PTVA-3. These results, in the form of tables or maps or both are provided to stakeholders, that is local authorities, emergency managers, long-term planners, etc., to mitigate tsunami impact. Though these indices are derived in totally different ways and contain somewhat different information, they both aim to rank buildings on the basis of an index broadly measuring the consequences of a tsunami attack, and this is provided in a 5-degree scale. This enables one to assume a one-to-one correspondence between the SCHEMA Dx and the PTVA-3 PD. Hence, after assigning integer values to Dx according to the trivial scheme D1 = 1, D2 = 2, etc., one can compare results by quantifying the discrepancies through the simple difference Dx-PD. This is mapped in Fig. 11 and summarized through the histogram of Fig. 12.

The difference distribution of the histogram (Fig. 12) is centered on zero, meaning that in most cases Dx and PD are found to be equal. However, it is

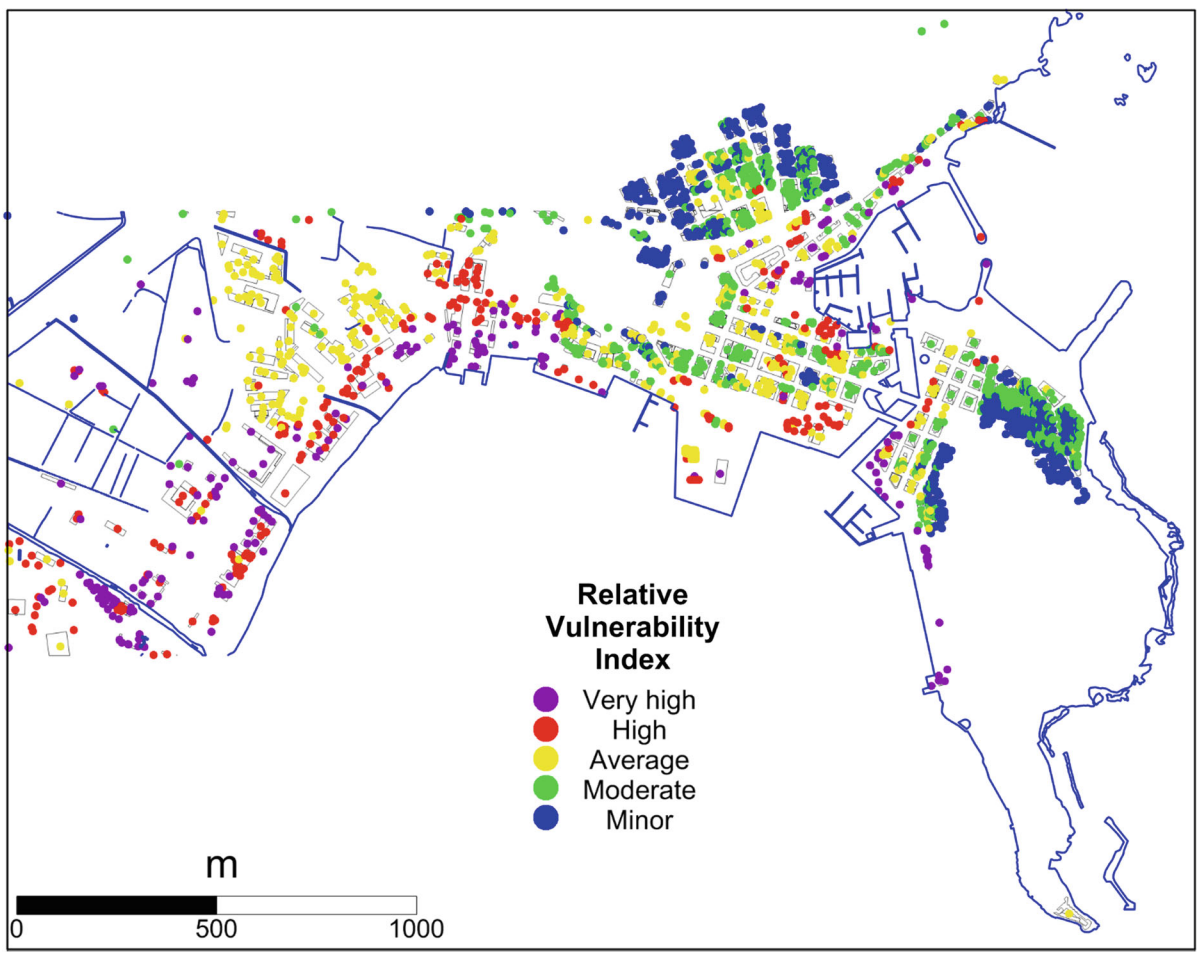

Figure 10
Damage level of buildings for an inundation level of 5 m calculated through the relative vulnerability index *Rv* of the PTVA-3 model

not symmetric, but strongly left tailed, revealing that in many cases the SCHEMA Dx is smaller than the corresponding PTVA-3 PD and in very few cases the opposite occurs. Most discrepancies are limited to 1 unit, and exceptionally they are 2 or 3 units, but never 4. The map of the differences reveals that 0-differences are concentrated in Ortigia and in the quarter of Santa Lucia, and that higher discrepancies (−2 and even −3) can be found in the Umbertin quarter, but mostly along the northern and coastal belt of Siracusa Bay, where ground level is lower. Further, notice that the few positive strong differences (+2) are concentrated in the industrial-commercial area inland.

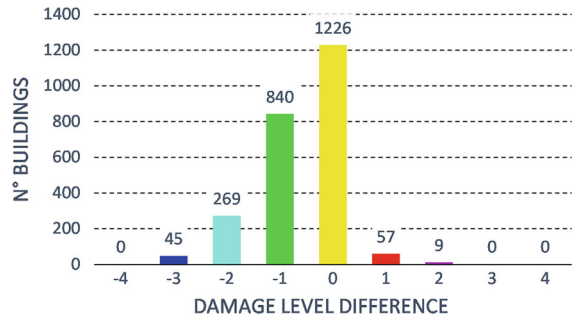

Figure 12
SCHEMA vs. PTVA-3 damage level for a 5-m inundation level. Differences are computed via the formula Dx (SCHEMA)−PD (PTVA-3)

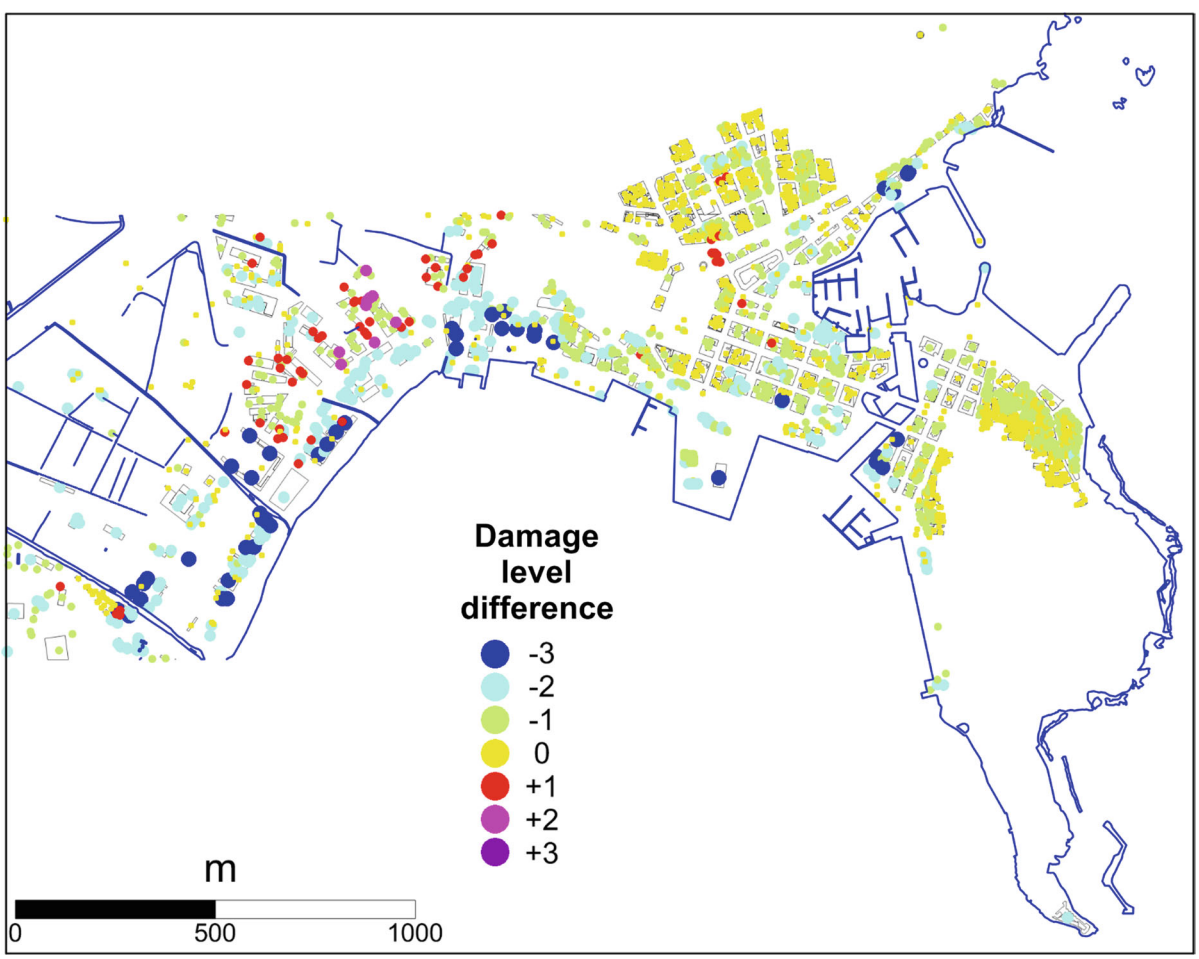

Figure 11
SCHEMA vs. PTVA-3 damage to buildings for a 5-m inundation level. Difference is computed via the formula Dx (SCHEMA)−PD (PTVA-3)

9. Discussion and Conclusions

The main aim of this paper was to apply different models to estimate vulnerability and damage to buildings under tsunami attack and to identify analogies and discrepancies in the result also as a basis to evaluate uncertainties. The methods we selected for this comparative study are SCHEMA and PTVA-3 and the main reasons for this choice is that they are well known in the specialized literature through a series of recent applications and that they are examples of two different basic approaches. The former (SCHEMA) is quantitative in nature and representative of all those methods where (a) buildings vulnerability classification is founded on a few engineering structural properties of the edifices and (b) damage levels derive from fragility curves obtained from field data in areas hit by tsunami floods. The second (PTVA-3) is more qualitative, and more depending on subjective judgements: it considers many more properties of the buildings and of the surrounding environment and provides scores that are combined together to produce indices that in turn can be further combined to give the final results. This latter scheme has the advantage that a lot of features (attributes) can be scored and used in the evaluation, but also the disadvantage that it has no value until attributes, parameters (weights), and algorithms are tested and calibrated on real cases. It is worth mentioning that testing and calibration of the PTVA-3 model was done also for the case of a recent tsunami in Stromboli, that is in a place not far from the area of Siracusa (Dall'Osso *et al.* 2010).

The area of application, i.e., the town of Siracusa, was selected because it is a very important town, also included in the list of UNESCO World Heritage Sites since 2005, that is located on a coastal region threatened by big and damaging tsunamis. A further reason for selecting Siracusa is that the Sicily region over recent years (this is the Italian region where Siracusa is located) has systematically built a very rich and valuable database with thematic layers given in the form of digital maps with a sophisticated level of detail (1:2000 CTN sheets), that made it possible to produce an inventory of the constructions suitable for vulnerability analysis.

As described and shown in the previous sections, the two models go along different paths that have only two points of crossing where inter-comparison is possible: (1) the buildings classification of SCHEMA can be put in parallel with the PTVA-3 building vulnerability index Bv; (2) the damage level to buildings of SCHEMA can be compared to the PTVA-3 index PD. The comparison was carried out under the hypothesis that the sea level rises uniformly (bath-tub assumption) by 5 m. This over-simplification is justified because the main focus is on the behavior of the models and serves to decouple vulnerability and damage evaluations from hazard assessments. A more specific study where the inundation level is heterogeneous will be carried out in the town when tsunami hazard will be estimated properly (see e.g., the exemplary study by Pagnoni *et al.* 2015, conducted for the town of Alexandria) and more information on the expected inundation area is available.

The joint evaluation of the buildings vulnerability shows that it is not possible to establish a one-to-one correspondence between the 5 building classes of SCHEMA, from A to E, and the 4 populated classes of Bv, from 2 to 5 (see Table 9). It seems that only class C can be assimilated to $Bv = 4$, since more than 91 % of class C entities are also attributed $Bv = 4$. The other classes show a larger dispersion: class A and class B distribute 73 % in $Bv = 5$ and 27 % in $Bv = 4$; class D distributes mostly in $Bv = 4$ (56 %) and $Bv = 3$ (39 %), and eventually class E is dispersed between $Bv = 3$ (23 %) and $Bv = 2$ (77 %). The fact that most categories of SCHEMA split in two categories of Bv, though with one prevailing, means that the two classifications are different and cannot be reconciled in a simple way. One can only recognize a rough correlation by stating that, when one goes from class A to class E, the corresponding value of Bv is expected to decrease from 5 to 2.

The analysis of damage to buildings is carried out by connecting the SCHEMA damage levels from D1 to D5 to the PTVA-3 index PD (see Figs. 9, 10, 11, 12). It was observed that for most buildings the two models provide coincident indices, but that it is also frequent the case that SCHEMA computes a smaller level of damage than PTVA-3 (see the difference histogram of Fig. 12). Table 10 shows the frequency

Table 10

SCHEMA damage levels D1–D5 compared to the PTVA-3 damage from "minor" (PD = 1) to "very high" (PD = 5)

SCHEMA	D1	%	D2	%	D3	%	D4	%	D5	%	Total
PTVA-3											
1	767	61	4	0.5	0	0	0	0	0	0	771
2	433	34	263	32	4	2.5	0	0	0	0	700
3	60	5	353	43.5	53	32.5	29	35	9	7	504
4	0	0	148	11	45	27.6	44	54	20	16	257
5	0	0	45	3	61	37.4	9	11	99	77	214
Total	1260		813		163		82		128		2446

The numbers (5, 4,…,1) in the first column denote the level of damage (PD) provided by PTVA-3 method. The assumed inundation level is 5 m

distribution of damage in a two-entry table of Dx vs. PD, and is analogous to Table 9 concerning vulnerability. In a perfect one-to-one correspondence the frequency matrix should contain only diagonal elements different from zero. What is seen instead is that diagonal elements tend to be the larger, which supports a general correspondence between Dx and PD, but this correspondence is "spoiled" by three main features: (1) the damage level D2 peaks on PD = 3; (2) the damage level D3, more than pointing to PD = 3, extends almost equally on the broad range PD = 3–5; (3) the diagonal elements of the central classes D2–D4 are rather low (not exceeding 54 %) and only for the extreme classes D1 and D5 they go beyond 60 %. The observation that the estimated damage Dx for a building is usually equal to or smaller than the estimated PD is also confirmed by Table 10 where it is clear that frequencies below the diagonal are larger than frequencies above. But Table 10 reveals that this is mostly due to the misplacement of the peak of the D2 column that is located below the diagonal suggesting a correspondence between D2 and PD = 3.

In conclusion, like for the vulnerability analysis, a perfect correlation between the damage level of SCHEMA and the PD index of PTVA-3 is not supported by our analysis, but only a rough correlation, by which we mean that usually if a building has an assessed damage level larger than another, it is expected that its PD is also larger. A less detailed damage grouping, however, could improve the correlation. From analyzing the matrix of Table 10, it is seen that a three-degree damage scale ND1-ND3,

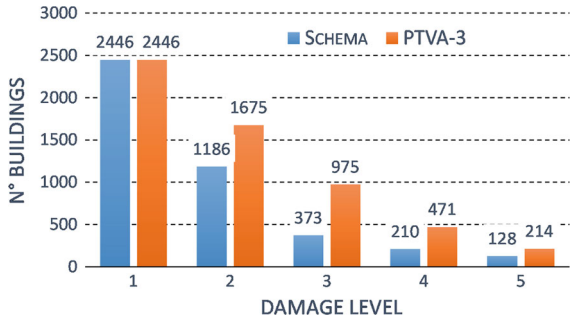

Figure 13
Complementary cumulative damage-level distributions of SCHEMA and PTVA-3 models for a 5-m sea level increase

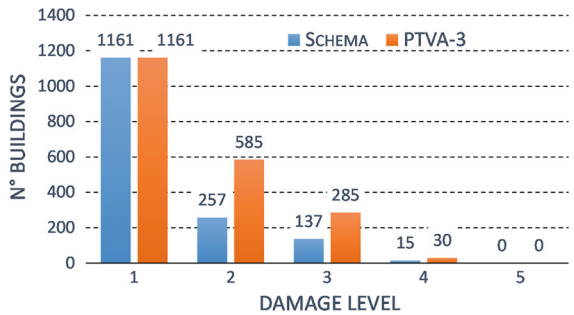

Figure 14
Complementary cumulative damage-level distributions of SCHEMA and PTVA-3 models for a 3-m tsunami inundation

where NDx denotes a New Damage level, could better correspond to a three-degree NPD with range 1–3 (with analogously NPD designating a New PTVA-3 Damage index), if the following grouping is made: ND1 equivalent to D1, ND2 containing from D2 to D4, and ND3 equivalent to D5; likewise

NPD = 1 equivalent to PD = 1, NPD = 2 including from PD = 2 to PD = 4, and NPD = 3 equivalent to PD = 5. This 3-degree scale could provide more consistent results between the two models.

So far our discussion was based on analyses concerning the 5-m inundation level. But our database is suitable for evaluation of any level of inundation less than 5 m, since in this case the corresponding inundation area is contained in the 5-m flooding zone, and therefore the corresponding inventoried buildings are simply a subset of the one already analyzed. In addition to the 5-m level, we have considered also 3- and 1-m levels of inundation, which reduced the number of constructions falling in the flooded area, respectively, to 1161 and to 57 (see Fig. 4). The purpose is to see if observations made for the 5-m sea level increase apply also to lower levels of inundation, that is for smaller tsunamis. The results are illustrated in Figs. 13, 14, 15 and in Tables 11 and 12. Figures provide the complementary cumulative frequency distribution (CCFD) of the damage level side by side with the CCFD of PD for the three assumed levels of inundation. In all cases the SCHEMA CCFD is found to decay much quicker than the PTVA-3 CCFD, which means that for all inundation cases Dx is found to be equal or smaller than the corresponding PD. Even the two-entry matrices given in Tables 11 and 12 (corresponding to 3- and 1-m inundation levels, respectively) support what was found for the 5-m inundation level.

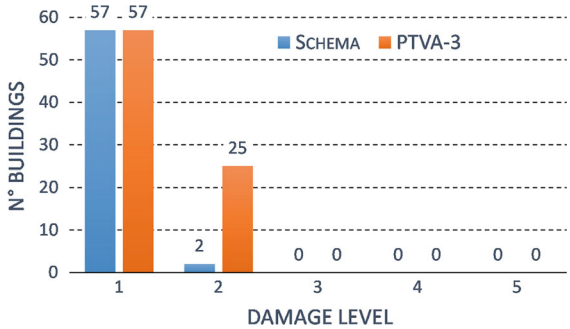

Figure 15
Complementary cumulative damage-level distributions of SCHEMA and PTVA-3 models for a 1-m tsunami flooding

Table 11

SCHEMA damage levels D1–D5 compared to the PTVA-3 damage from "minor" (PD = 1) to "very high" (PD = 5)

SCHEMA	D1	%	D2	%	D3	%	D4	%	D5	%	Total
PTVA-3											
1	575	63	1	1	0	0	0	0	0	0	576
2	241	27	46	39	13	11	0	0	0	0	300
3	88	10	66	56	100	82	1	7	0	0	255
4	0	0	7	4	9	7	14	93	0	0	30
5	0	0	0	0	0	0	0	0	0	0	0
Total	904		120		122		15		0		1161

The assumed inundation level is 3 m

Table 12

SCHEMA damage levels D1–D5 compared to the PTVA-3 damage from "minor" (PD = 1) to "very high" (PD = 5)

SCHEMA	D1	%	D2	%	D3	%	D4	%	D5	%	Total
PTVA-3											
1	32	58	0	0	0	0	0	0	0	0	32
2	23	42	2	100	0	0	0	0	0	0	25
3	0	0	0	0	0	0	0	0	0	0	0
4	0	0	0	0	0	0	0	0	0	0	0
5	0	0	0	0	0	0	0	0	0	0	0
Total	55		2		0		0		0		57

The assumed inundation level is 1 m

The main three conclusions following the above discussion are that (1) the two models provide tsunami damage pictures that are discrepant, although increased damage in one model usually implies an increased PD in the other; (2) consistency between the models can be improved if the five-degree scale is replaced suitably by a three-degree scale of damage; (3) the level of inundation has no substantial influence on the previous two statements.

Acknowledgments

The authors are indebted to Dr Francesco Rallo who provided some of the data and some preliminary analyses for this research. The research conducted in this paper is the follow-up of a research initiated during the European FP6 project TRANSFER (Contract No. 037058). It is mostly financed by the ongoing FP7 project ASTARTE—"Assessment, Strategy And Risk Reduction for 740 Tsunamis in Europe" (FP7-ENV2013 6.4-3, Grant 603839).

References

Aloisi, M., Bruno, V., Cannavò, F., Ferranti, L., Mattia, M., Monaco, C., and Palano, M. (2013). *Are the source models of the Messina Straits earthquake reliable? Insights from a novel inversion and a sensitivity analysis of levelling data*. Geophys. J. Int., *192*, 1025–1041.

Amato, A., Azzara, R., Basili, A., Chiarabba, C., Cocco, M., Di Bona, M., and Selvaggi, G. (1995). *Main shock and aftershocks of the December 13, 1990 Eastern Sicily earthquake*. Annali di Geofisica, *38*, 255–266.

Argnani, A., and Bonazzi, C. (2005). *Malta Escarpment fault zone offshore eastern Sicily: Pliocene-Quaternary tectonic evolution based on new multichannel seismic data*. Tectonics, *24*, 1–12. doi:10.1029/2004TC001656.

Argnani, A., Chiocci, F.L., Tinti, S., Bosman, A., Lodi, M.V., Pagnoni, G., and Zaniboni, F. (2009). *Comment on "On the cause of the 1908 Messina tsunami, southern Italy" by Andrea Billi et al.* Geophys. Res. Lett. *36*, 3–5. doi:10.1029/2009GL037332.

Argnani, A., Armigliato, A., Pagnoni, G., Zaniboni, F., Tinti, S., and Bonazzi, C. (2012). *Active tectonics along the submarine slope of south-eastern Sicily and the source of the 11 January 1693 earthquake and tsunami*. Nat. Hazards Earth Syst. Sci., *12*, 1311–1319.

ASV, Relazione dell'Inquisitore di Malta F. d'Acquaviva al Segretario di Stato Cardinale Spada sui danni causati a Malta e in Sicilia dal terremoto dell'11 gennaio 1693 (Archivio Segreto Vaticano, Segreteria di Stato, Inquisizione, Malta 1693).

Atillah, A., El Hadani, D., Moudni, H., Lesne, O., Renou, C., Mangin, A., and Rouffi, F. (2011). *Tsunami vulnerability and damage assessment in the coastal area of Rabat and Sale, Morocco*. Nat. Hazards Earth Syst. Sci., *11*, 3397–3414.

Baratta, M., I terremoti d'Italia. Saggio di storia, geografia e bibliografia sismica italiana con 136 sismocartogrammi (Arnaldo Forni Editore, 1901).

Baratta, M. (1910). La catastrofe sismica calabro-messinese del 28 dicembre 1908, Relazione alla Società Geografica Italiana.

Barbano, M. S., Rigano, R., Cosentino, M. and Lombardo G. (2001). *Seismic history and hazard in some localities of south-eastern Sicily*. Boll. Geof. Teor. Appl., *42*, 107–120.

Basili, R., Valensise, G., Vannoli, P., Burrato, P., Fracassi, U., Mariano, S., Tiberti, M.M., and Boschi, E. (2008). *The Database of Individual Seismogenic Sources (DISS), version 3: summarizing 20 years of research on Italy's earthquake geology*. Tectonophysics *453*, 20–43. doi:10.1016/j.tecto.2007.04.014.

Basili, R., Kastelic, V., Demircioglu, M.B., Garcia Moreno, D., Nemser, E.S., Petricca, P., Sboras, S.P., Besana-Ostman, G.M., Cabral, J., Camelbeek, T., Caputo, R., Danciu, L., Domac, H., Fonseca, J., Garcia-Mayofomo, J., Giardini, D., Glavatovic, B., Gulen, L., Ince, Y., Pavlides, S., Sestyan, K., Tarabusi, G., Tiberti, M.M., Utkucu, M., Valensise, G., Vanneste, K., Vilanova, S., and Wössner, J. (2013). The European Database of Seismogenic Faults (ESDF) compiled in the frame work of the Project SHARE. http://diss.rm.ingv.it/share-edsf/. doi:10.6092/INGV.IT-SHARE-EDSF.

Bianca, M., Monaco, C., Tortorici, L., and Cernobori, L. (1999). *Quaternary normal faulting in southeastern Sicily (Italy): a seismic source for the 1693 large earthquake*. Geophys. J. Int., *139*, 370–394.

Billi, A., Funiciello, R., Minelli, L., Faccenna, C., Neri, G., Orecchio, B., and Presti, D. (2008). *On the cause of the 1908 Messina tsunami, southern Italy*. Geophys. Res. Lett. *35*, 1–5. doi:10.1029/2008GL033251.

Billi A., Minelli L., Orecchio B., and Presti D. (2010). *Constraints to the Cause of Three Historical Tsunamis (1908, 1783, and 1693) in the Messina Straits Region, Sicily, Southern Italy*. Seism. Res. Lett. (Seism. Soc. Am.), *81*, 907–915.

Birkmann, J., and Fernando, N. (2008). *Measuring revealed and emergent vulnerabilities of coastal communities to tsunami in Sri Lanka*. Disasters, *32*, 82–105.

Boccone, P, Intorno il terremoto della Sicilia seguito l'anno 1693 (Museo di Fisica, Venezia 1697).

Boschi, E., Guidoboni, E., Ferrari, G., Valensise, G., and Gasperini, P., Catalogo dei forti terremoti in Italia dal 461 a.C. al 1990 (2) (I.N.G.-S.G.A, Roma 1997).

Bottone, D., De immani Trinacriae terraemotu. Idea historico-physica, in qua non solum telluris concussiones transactae recensentur, sed novissimae anni 1717. (ex typogr. reg. & camer. haered. de Amico, Messanae 1718).

Brizuela, B., Armigliato, A., and Tinti, S. (2014). *Assessment of tsunami hazard for the American Pacific coast from southern Mexico to northern Peru*. Nat. Hazards Earth Syst. Sci. *14*, 1889–1903. doi:10.5194/nhess-14-1889-2014.

Burbidge, D., Cummins, P.R., Mleczko, R., and Thio, H.A. (2008). *Probabilistic tsunami hazard assessment for Western Australia*. Pure Appl. Geophys, *165*, 2059–2088.

Burgos, A., Distinta relazione avuta per lettera del P. Alessandro Burgos scritta ad un suo amico, che contiene le notizie fin'ora avute de danni cagionati in Sicilia da tremuoti a 9 e 11 gennaio 1693 (Palermo 1693).

Camarasa Belmonte, A.M., López-García, M.J. and Soriano-García, J. (2011). *Mapping temporally-variable exposure to flooding in small Mediterranean basins using land-use indicators*. Appl. Geogr., *31*, 136–145.

Cita, M.B., Rimoldi, B. (1997). *Geological and geophysical evidence for a holocene tsunami deposit in the Eastern Mediterranean deep-sea record*. J. Geodyn. *24*, 293–304. doi:10.1016/S0264-3707(96)00030-0.

Dall'Osso, F., Gonella, M., Gabbianelli, G., Withycombe, G., and Dominey-Howes, D. (2009a). *A revised (PTVA) model for assessing the vulnerability of buildings to tsunami damage*. Nat. Hazards Earth Syst. Sci., *9*, 1557–1565.

Dall'Osso, F., Gonella, M., Gabbianelli, G., Withycombe, G., and Dominey-Howes, D. (2009b). *Assessing the vulnerability of buildings to tsunami in Sydney*. Nat. Hazards Earth Syst. Sci., *9*, 2015–2026.

Dall'Osso, F., Maramai, A., Graziani, L., Brizuela, B., Cavalletti, A., Gonella, M., and Tinti, S. (2010). *Applying and validating the PTVA-3 Model at the Aeolian Islands, Italy: assessment of the vulnerability of buildings to tsunamis*. Nat. Hazards Earth Syst. Sci., *10*, 1547–1562.

De Martini, P.M., Barbano, M.S., Smedile, A., Gerardi, F., Pantosti, D., Del Carlo, P., and Pirrotta, C. (2010). *A 4000 yrs long record of tsunami deposits along the coast of the Augusta Bay (eastern Sicily, Italy): paleoseismological implications*. Marine Geology, *276*, 42–57.

De Martini, P.M., Barbano, M.S., Pantosti, D., Smedile, A., Pirrotta, C., Del Carlo, P., and Pinzi, S. (2012). *Geological evidence for paleotsunamis along eastern Sicily (Italy): an overview*. Nat. Hazards Earth Syst. Sci., *12*, 2569–2580.

Dominey-Howes, D., and Papathoma, M. (2007). *Validating a Tsunami Vulnerability Assessment Model (the PTVA Model) Using Field Data from the 2004 Indian Ocean Tsunami*. Nat. Hazards, *40*, 113–136.

DISS Working Group (2010). Database of Individual Seismogenic Sources (DISS), Version 3.1.1: A compilation of potential sources for earthquakes larger than M 5.5 in Italy and surrounding areas. http://diss.rm.ingv.it/diss/, © INGV 2010–Istituto Nazionale di Geofisica e Vulcanologia–All rights reserved; doi:10.6092/INGV.IT-DISS3.1.1.

Eckert, S., Jelinek, R., Zeug, G., and Krausmann, E. (2012). *Remote sensing-based assessment of tsunami vulnerability and risk in Alexandria, Egypt*. Appl. Geogr., *32*, 714–723.

Favalli, M., Boschi, E., Mazzarini, F., and Pareschi, M.T. (2009). *Seismic and landslide source of the 1908 Straits of Messina tsunami (Sicily, Italy)*. Geophys. Res. Lett. *36*, 1–6. doi:10.1029/2009GL039135.

Fritz, H.M., Phillips, D.A., Okayasu, A., Shimozono, T., Liu, H.J., Mohammed, F., Skanavis, V., Synolakis, C.E., and Takahashi, T. (2012). *The 2011 Japan tsunami current velocity measurements from survivor videos at Kesennuma Bay using LiDAR*. Geophys. Res. Lett. *39*, 1–6. doi:10.1029/2011GL050686.

Gardi, A., Valencia, N., Guillande, R., and André, C. (2011). *Inventory of uncertainties associated with the process of tsunami damage assessment on buildings (SCHEMA FP6 EC co-funded project)*. Nat. Hazards Earth Syst. Sci., *11*, 883–893.

Geist, E.L., and Parsons, T. (2006). *Probabilistic analysis of tsunami hazards*. Natural Hazards, *37*, 277–314.

Gerardi, P., Barbano, M.S., De Martini, P.M., and Pantosti, D. (2008). *Discrimination of Tsunami Sources (Earthquake versus Landslide) on the Basis of Historical Data in Eastern Sicily and Southern Calabria*. Bull. Seism. Soc. Am., *98*, 2795–2805.

Grilli, S.T., Harris, J., and Tajalli Bakhsh, T., 2011. Literature Review of Tsunami Sources Affecting Tsunami Hazard Along the US East Coast, NTHMP Progress report, Res. Rept. CACR-11-08, Center for Applied Coastal Research, University of Delaware, Newark.

Guidoboni, E., Comastri, A., and Traina, G., Catalogue of Ancient Earthquakes in the Mediterranean Area up to 10th Century (Istituto Nazionale di Geofisica, Roma 1994).

Guidoboni E., Ferrari G., Mariotti D., Comastri A., Tarabusi G., and Valensise G. (2007). CFTI4Med, Catalogue of Strong Earthquakes in Italy (461 B.C.–1997) and Mediterranean Area (760 B.C.–1500). INGV-SGA. http://storing.ingv.it/cfti4med/.

Gutscher, M.A., Roger J., Baptista, M.A., Miranda, J.M., and Tinti, S. (2006). *Source of the 1693 Catania earthquake and tsunami (southern Italy): new evidence from tsunami modelling of a locked subduction fault plane*. Geophys. Res. Lett. *33*. doi:10.1029/2005GL025442.

Kastens, K. A. and Cita, M. B. (1981). *Tsunami-induced sediment transport in the abyssal Mediterranean Sea*. Geol. Soc. Am. Bull., *92*, 845–857.

Leone, F., Lavigne, F., Paris, R., Denain, J.C., and Vinet, F. (2010). *A spatial analysis of the December 26th, 2004 tsunami-induced damages: lessons learned for a better risk assessment integrating buildings vulnerability*. Appl. Geogr., *31*, 363–375.

McCoy, F.W., and Heiken, G. (2000). *Tsunami Generated by the Late Bronze Age Eruption of Thera (Santorini), Greece*. Pure Appl. Geophys., *157*, 1227–1256.

Martinelli, G. (1909). *Osservazioni preliminari sul terremoto calabro-messinese del mattino del 28 dicembre 1908*, Bollettino Bimensuale della Società Meteorologica Italiana, serie III, *28*, 3–11.

Mercalli, G., Contributo allo studio del terremoto calabro-messinese del 28 dicembre 1908 (Cooperativa Tipografica, Napoli 1909).

Monaco, C., and Tortorici, L. (2000). Active faulting in the Calabrian arc and eastern Sicily. J. Geodyn. 29, 407–424.

Pagnoni, G., Armigliato, A., and Tinti, S. (2015). *Scenario-based assessment of buildings damage and population exposure due to tsunamis for the town of Alexandria, Egypt*. Nat. Hazards Earth Syst. Sci., submitted revision.

Papadopoulos, G. A., and Dermetzopoulos, T. (1998). *A tsunami risk assessment pilot study in Heraklion, Crete*. Natural Hazards, *18*, 91–118.

Papathoma, M., Dominey-Howes, D., Zong, Y., and Smith, D. (2003). *Assessing tsunami vulnerability, an example from Herakleio, Crete*. Nat. Hazards Earth Syst. Sci., *3*, 377–389.

Papathoma, M., and Dominey-Howes, D. (2003*). Tsunami vulnerability assessment and its implications for coastal hazard analysis and disaster management planning, Gulf of Corinth, Greece*. Nat. Hazards Earth Syst. Sci., *3*, 733–747.

Piatanesi, A., and Tinti, S. (1998). *A revision of the 1693 eastern Sicily earthquake and tsunami*, J. Geophys. Res. *103*, 2749–2758.

Piatanesi, A., Tinti, S., and Bortolucci, E. (1999). *Finite-element simulations of the 28 December 1908 Messina Straits (southern Italy) tsunami*. Phys. Chem. Earth Part A. *24*, 145–150.

Piatanesi, A., Lorito, S., and Romano, F., Il grande maremoto del 1908: analisi e modellazione, In Il Terremoto e il Maremoto del 28 dicembre 1908: analisi sismologica, impatto, prospettive (ed.

Bertolaso, G., Boschi, E., Guidoboni, E., Valensise, G.) (INGV-DPC, Roma-Bologna 2008).

Platania, G. (1909a). *Il maremoto dello stretto di Messina del 28 dicembre 1908*. Boll. Soc. Sism. Ital., *13*, 369–458.

Platania, G. (1909b). *I fenomeni marittimi che accompagnarono il terremoto di Messina del 28 dicembre 1908*, Rivista Geografica Italiana, *16*, 154–161.

Polonia, A., Bonatti, E., Camerlenghi, A., Lucchi, R.G., Panieri, G., and Gasperini, L. (2013). *Mediterranean megaturbidite triggered by the AD 365 Crete earthquake and tsunami*. Sci. Rep. *3*, 1285. doi:10.1038/srep01285.

Reese, S., Cousins, W.J., Power, W.L., Palmer, N.G., Tejakusuma, I.G., and Nugrahadi, S. (2007). *Tsunami vulnerability of buildings and people in south Java–field observations after the July 2006 Java tsunami*. Nat. Hazards Earth Sys., *7*, 573–589.

Ribeiro, J., Silva, A., and Leitão, P. (2011). *High resolution tsunami modelling for the evaluation of potential risk areas in Setúbal (Portugal)*. Nat. Hazards Earth Syst. Sci., *11*, 2371–2380.

Ridente, D., Martorelli, E., Bosman, A., and Chiocci, F.L. (2014). *High-resolution morpho-bathymetric imaging of the Messina Strait (Southern Italy). New insights on the 1908 earthquake and tsunami*. Geomorphology, *208*, 149–159.

Ryan W.B.F., and Heezen B.C. (1965). *Ionian Sea submarine canyons and the 1908 Messina turbidity current*. Geol. Soc. Am. Bull., *76*, 915–932.

Sirovich, L., and Pettenati, F. (1999). *Seismotectonic outline of South-Eastern Sicily: an evaluation of available options for the earthquake fault rupture scenario*. J. Seismology, *3*, 213–233.

Scicchitano, G., Monaco, C., and Tortorici, L. (2007). *Large boulder deposits by tsunami waves along the Ionian coast of south-eastern Sicily (Italy)*. Mar. Geol. *238*, 75–91.

Scicchitano, G., Costa, B., Di Stefano, A., Longhitano, S.G., and Monaco, C. (2010). *Tsunami and storm deposits preserved within a ria-type rocky coastal setting (Siracusa, SE Sicily)*. Zeitschrift für Geomorphol. Suppl. Issues *54*, 51–77. doi:10.1127/0372-8854/2010/0054S3-0019.

Shaw, B., Ambraseys, N.N., England, P.C., Floyd, M.A., Gorman, G.J., Higham, T.F.G., Jackson, J.A., Nocquet, J.M., Pain, C.C. and Piggott, M.D. (2008). *Eastern Mediterranean tectonics and tsunami hazard inferred from the AD 365 earthquake*. Nat. Geosci. *1*, 268–276.

Smedile, A., De Martini, P.M., and Pantosti, D. (2012). *Combining inland and offshore paleotsunamis evidence: the Augusta Bay (eastern Sicily, Italy) case study*. Nat. Hazards Earth Syst. Sci., *12*, 2557–2567.

Sørensen, M.B., Spada, M., Babeyko, A., Wiemer, S., and Grünthal, G. (2012). *Probabilistic tsunami hazard in the Mediterranean Sea*. J. Geophys. Res. Solid Earth *117*, 1–15. doi:10.1029/2010JB008169.

Tinti, S. (1991). *Assessment of tsunami hazard in the Italian Seas*, Nat. Hazards, *4*, 267–283.

Tinti, S., and Armigliato, A., Tsunamigenic earthquakes, In Problems in Geophysics for the New Millennium (ed. Boschi E., Ekström G., Morelli A.) (Editrice Compositori, Bologna 2000) pp. 27–46.

Tinti, S., and Armigliato, A., Impact of large tsunamis in the Messina Straits, Italy: the case of the 28 December 1908 tsunami, In Tsunami Research at the End of a Critical Decade (ed. Hebenstreit, G.T.) (Kluwer, Dordrecht 2001) pp. 139–162.

Tinti, S., Armigliato, A., and Bortolucci, E. (2001). Contribution of tsunami data analysis to constrain the seismic source: the case of the 1693 eastern Sicily earthquake. J. Seismology, 5, 41-61.

Tinti S., Maramai A., and Graziani L. (2004). *The new catalogue of the Italian tsunamis*, Nat. Hazards, *33*, 439–465.

Tinti, S., Armigliato, A., Pagnoni, G., and Zaniboni F. (2005a). *Scenarios of giant tsunamis of tectonic origin in the Mediterranean*. ISET Journal of Earthquake Technology, *42*, 171–188.

Tinti, S., Manucci, A., Pagnoni, G., Armigliato, A., and Zaniboni F., (2005b). *The 30th December 2002 tsunami in Stromboli: sequence of the events reconstructed from the eyewitness accounts*. Nat. Hazards Earth Syst. Sci., *5*, 763–775.

Tinti, S., Pagnoni, G., and Zaniboni F. (2006). *The landslides and tsunamis of 30th December 2002 in Stromboli analysed through numerical simulations*. Bull. Volcanol., *68*, 462–479.

Tinti, S., Argnani, A., Zaniboni, F., Pagnoni, G., and Armigliato, A. (2007). Tsunamigenic potential of recently mapped submarine mass movements offshore eastern Sicily (Italy): numerical simulations and implications for the 1693 tsunami. Abstract n.8235, IUGG XXIV General Assembly.

Tinti, S., Armigliato, A., Pagnoni, G., Tonini, R., and Zaniboni, F., Atlante delle zone esposte al rischio di maremoto nell'area di Catania (Compositori, Bologna 2010).

Tinti, S., Tonini, R., Bressan, L., Armigliato, A., Gardi, A., Guillande, R., Valencia, N., and Scheer, S. (2011). Handbook of tsunami hazard and damage scenarios. JRC Scientific and Technical Reports, pp. 1–41, doi: 10.2788/21259.

Tonini, R., Armigliato, A., Pagnoni, G., Zaniboni, F., and Tinti, S., (2011). *Tsunami hazard for the city of Catania, eastern Sicily, Italy, assessed by means of Worst-case Credible Tsunami Scenario Analysis (WCTSA)*. Nat Hazards Earth Syst Sci, *11*, 1217–1232.

Valencia, N., Gardi, A., Gauraz, A., Leone, F., and Guillande R. (2011). *New tsunami damage functions developed in the framework of SCHEMA project: application to European-Mediterranean coasts*. Nat. Hazards Earth Syst. Sci., *11*, 2835–2846.

Valensise, G., and Pantosti, D. (1992). *A 125 kyr-long geological record of seismic source repeatability: the Messina Straits (southern Italy) and the 1908 earthquake (Ms 7 1/2)*. Terra Nova, *4*, 472–483.

Zaniboni, F., Armigliato, A., Pagnoni, G., and Tinti, S. (2014). Earthquake or landslide-tsunami? Discriminating the source type by the effects on the coast. Abstract presented at the EGU General Assembly 2014, EGU2014-10025, Geophysical Research Abstracts, Vol. 16.

(Received December 3, 2015, accepted February 24, 2016, Published online March 14, 2016)